LOCAL APPROXIMATIONS OF THE STEKLOV POINCARE OPERATOR FOR A CLASS OF ELLIPTIC OPERATORS, AND DOMAIN DECOMPOSITION METHODS.

Y. Achdou [1] & F.Nataf[2]

Abstract

Many implicit Navier Stokes solvers involve the discretization of an elliptic partial differential equation of the type $-\Delta u + \eta u = f$, where η is a large positive parameter. The discretization studied here is the mortar finite element method, a domain decomposition method allowing non matching meshes at subdomains interfaces. Two kinds of improvements are proposed here in order to reduce the condition number of the corresponding linear systems : the first one lies on building preconditioners by approximating Steklov-Poincaré operators on subdomains boundaries by second order partial differential operators; the second one consists in making a non standard choice of jump operators at subdomains interfaces. Both ideas are tested numerically.

CONTENT

[1] CMAP,Ecole Polytechnique: achdou [?]mapx.polytechnique.fr

[2] CMAP,Ecole Polytechnique: nataf [?]mapx.polytechnique.fr

0 INTRODUCTION

This work on preconditioners has been motivated by the development of a solver in 2 dimensions for the Navier Stokes equations in the stream function-vorticity formulation (see [2]) using a non-conforming nonoverlapping domain decomposition method based on Q_1 finite elements, namely the *mortar* element method. This method was first introduced by C.Bernardi, Y.Maday, A.Patera in [6].

Each time iteration of the Navier Stokes solver is split into a convection and a diffusion steps. The convection is treated by the characteristic Galerkin method (see [2] and references therein). The diffusion step is the resolution of the following fourth order elliptic problem in ψ, namely the following generalized Stokes problem :

$$\begin{aligned} &-\Delta\omega + \eta\omega = f, \quad -\Delta\psi = \omega \quad \text{ in } \Omega, \\ &\frac{\partial\psi}{\partial n} = g_1, \quad \psi = g_2 \quad \text{ on } \partial\Omega. \end{aligned} \tag{0.1}$$

where $\eta = \frac{1}{\nu\delta t}$, ν is the viscosity, and δt the time step.

In fact, following the ideas of R. Glowinski and O. Pironneau, it is possible to replace this fourth order problem by four second order problems, at the cost of solving a capacitance problem on $\partial\Omega$. Such a method enables to solve numerically fourth order problems in a mixed way by using low order finite elements (here, Q_1 finite elements). For the sake of shortness, this method is not described in this paper : we refer to [12] for the original method and to [2] for a rather different implementation involving an integral equation. For the following, it is enough to know that each time step involves two Poisson problems for the stream function ψ of the type :

$$\begin{aligned} &-\Delta\psi = f \quad \text{ in } \Omega, \\ &\psi = g \quad \text{ on } \partial\Omega, \end{aligned} \tag{0.2}$$

and two Helmholtz problems for the vorticity ω of the type :

$$\begin{aligned} &-\Delta\omega + \eta\omega = f \quad \text{ in } \Omega, \\ &\omega = \xi \quad \text{ on } \partial\Omega. \end{aligned} \tag{0.3}$$

The above mentioned elliptic problems are discretized by the Q_1 mortar element method in the version introduced in [4], which will be briefly described in section 2. This method is essentially a domain decomposition method with nonoverlapping subdomains. It has the advantage to allow nonmatching grids at the interfaces beetween subdomains and therefore permits to use very simple structured meshes in each subdomain. The continuity constraint at subdomains interfaces is written in a weak form, and it will turn out that the discretization described in this paper is non conforming even if the grids are matched at interfaces.

Algebraically, after elimination of the degrees of freedom internal to subdomains, the method leads to linear systems of the following saddle point form :

$$\begin{pmatrix} S & B^T \\ B & 0 \end{pmatrix} \begin{pmatrix} V \\ \Lambda \end{pmatrix} = \begin{pmatrix} F \\ 0 \end{pmatrix} \tag{0.4}$$

where S is a block diagonal matrix (one block per subdomain) and B is a jump operator. The vector V corresponds to unknowns located on interfaces, and Λ is the vector of Lagrange multipliers. In fact, the block S_k corresponds to a discretized version of $\mathcal{S}_k$ the Steklov Poincaré of subdomain Ω_k :

$$\mathcal{S}_k : H^{\frac{1}{2}}(\partial\Omega_k) \to H^{-\frac{1}{2}}(\partial\Omega_k),$$
$$\mathcal{S}_k u = \frac{\partial v}{n},$$

where v is defined by :

$$-Deltav + \eta v = 0 \quad \text{in } \Omega_k,$$
$$v = u \quad \text{on } \partial\Omega_k.$$

In [1], algorithms and preconditioners were designed for the Laplace solver. The aim of this article is to try to improve the efficiency of this method for the Helmholtz operator, for large values of η. When η is large, we shall see that the Steklov Poincaré operator is not too far from being a local operator; this property will be extensively used in the following. Two methods will be presented.

1 The first one, (§2 and §3), consists in building a preconditioner by approximating the discrete Steklov Poincaré operator S_{kh} of subdomain Ω_k by a second order symmetric partial differential operator on $\partial\Omega_k$. The methodology is the following : first, the discrete Steklov Poincaré is diagonalised in a Fourier basis, as in [10] for example; then the local preconditioner is found by solving a 1D optimization problem.

2 The second one , (§4), rather new to our knowledge, lies on choosing properly the jump operator B in order to minimize the condition number of $B^T S^{-1} B$. This approach is in some sense related to techniques of artificial boundary conditions, see [11], [15].

Note that the proposed preconditioners do not involve solving additional elliptic problems in subdomains as those proposed in [8],[14],[9]. Of course, this approach will not supply condition numbers almost independant of the stepsize as it is the case in [8],[14],[9]. Their main advantage is rather that they hardly increase the computing cost per iteration and memory requirements. The other possible advantage is that they behave well when subdomains themselves become small (see [3]).

Section 1 is devoted to recalls on the mortar method of C.Bernardi, Y.Maday, A.Patera, and on an algorithm for solving (0.3), developped in [6]. In §2, an approximation of the Steklov Poincaré operator is derived by means of a continuous analysis. The same work is carried out in §3 directly at the discrete level, which improves the condition number especially when the grids present high aspect ratios, which is often the case when dealing with laminar flows at high Reynolds number. Numerical tests are given at the end of §3. In section 4, the other strategy of choosing a non standard jump operator is presented along with numerical tests.

NOTATIONS

With each finite element function f_h, we associate the vector F of its coordinates in the cannonical basis. Accordingly, with each operator L_h, we associate the matrix L .
Ω : domain of $\mathbb{R}^2$, divided into K non overlapping subdomains.
Ω_k : subdomain of Ω.
$\Gamma_{kl} = \bar{\Omega}_k \cap \bar{\Omega}_l$.
$\Gamma = \cup \Gamma_{kl}$.
$\mathcal{T}_{k,h}$: quadrangulation of Ω_k.
X_{kh} : Q_1 finite element space associated to Ω_k and $\mathcal{T}_{k,h}$. $X_h = \prod_{1 \le k \le K} X_{kh}$.
Tr_k : trace operator from Ω_k to $\partial\Omega_k$.
$Z_{kh} = Tr_k X_{kh}$.

W_h : space for the Lagrange multiplier in the mortar element method.
B_h : $X_h \to W_h'$: jump operator.
b_h : $X_h \times W_h \to \mathbb{R}$: bilinear form : $b_h(u_h, \mu_h) =< B_h u_h, \mu_h >$

1 RECALLS

1.1. Recalls on the mortar method

The methodology of the mortar method is the following :

- The domain is first decomposed into non overlapping subdomains.
- The continuous domain decomposition problem is written in a variational form .
- A Galerkin method is used to discretize the problem : for each subdomain, there is a discrete space (possibly of finite elements) and at each intersection of two subdomains, a " mortar function " is introduced to enforce matching conditions.

Notice that in general, such a methodology leads to nonconforming approximations, because the meshes need not match at subdomains'interfaces. We shall see that our implementation is never conforming.

1.1.a The geometry.

Let Ω be a bounded polygonal domain of $\mathbb{R}^2$, and let Ω_k be a partition of Ω into K non-overlapping open quadrilaterals :

$$\overline{\Omega} = \cup_{k=1}^{K} \overline{\Omega}_k \qquad \text{and} \qquad \Omega_k \cap \Omega_l = \emptyset \quad \text{if } k \neq l. \tag{1.1}$$

This restriction to polygonal domain and subdomains is made only for the sake of simplicity. In fact, in our simulations, the domain is not polygonal and neither are the subdomains, (we just require that $\forall k,\ \partial\Omega_k \cap \Omega$ is a made of straight segments).

We also suppose that the domain decomposition is geometrically conforming, which means that the intersection of two subdomains is either empty or a vertex or a whole edge. Note that this is an implementation choice and not a limitation of the mortar method. For any $1 \leq k < l \leq K$, let Γ_{kl} be the closed straight segment, possily degenerate : $\Gamma_{kl} = \overline{\Omega}_k \cap \overline{\Omega}_l$.

1.1. b The discretization

Let us consider the model elliptic problem in Ω : find u in $H_0^1(\Omega)$ such that

$$\forall v \in H_0^1(\Omega), \qquad \int_\Omega \nabla u \cdot \nabla v \ \mathrm{d}x + \eta \int_\Omega u\, v \ \mathrm{d}x = \int_\Omega f\, v \ \mathrm{d}x. \tag{1.2}$$

Following [6], let us introduce the space Y :

$$Y = \left\{ \mathbf{v} = (v_k)_{1\leq k\leq K},\ v_k \in H^1(\Omega_k),\ \forall l,k : \ |\Gamma_{kl}| \neq 0, \quad v_{k|_{\Gamma_{kl}}} = v_{l|_{\Gamma_{kl}}},\ v_{|\partial\Omega} = 0 \right\}. \tag{1.3}$$

The space Y is exactly $H_0^1(\Omega)$. Thus, problem (1.2) is equivalent to the following continuous variational problem : find $\mathbf{u} \in Y$ such that

$$\forall \mathbf{v} \in Y, \qquad \sum_{k=1}^{K} \int_{\Omega_k} \nabla u_k \cdot \nabla v_k \ \mathrm{d}x + \eta \sum_{k=1}^{K} \int_{\Omega_k} u_k\, v_k \ \mathrm{d}x = \sum_{k=1}^{K} \int_{\Omega_k} f\, v_k \ \mathrm{d}x. \tag{1.4}$$

We discretize this problem by means of a Galerkin method : to do it, with each $1 \leq k \leq K$, we associate a family of quadrangular finite element meshes $\mathcal{T}_{k,h}$ of Ω_k, with the classical regularity assumption for F.E.M., and we denote X_{kh} the related space of isoparametric Q^1 finite elements. We define by X_h the product space :

$$X_h = \prod_{1 \le k \le K} X_{kh}.$$

Note that we do not impose any matching conditions for the grids at subdomains interfaces. We now have to define a space of mortar functions : we denote by Tr_k the trace operator from $H^1(\Omega_k)$ onto $H^{1/2}(\partial\Omega_k)$. If $|\Gamma_{kl}| \neq 0$, let $\tilde{\tilde{W}}_{kl,h}$ be the space

$$\tilde{\tilde{W}}_{k,l,h} = \left\{ Tr_k v_{|\Gamma_{kl}}, \quad v \in X_{kh} \right\}, \tag{1.5}$$

of dimension $m_{k,l}$, (here, the number of vertices of $\mathcal{T}_{k,h}$ lying on Γ_{kl}) and let $n_{k,l} = max(m_{k,l}, m_{l,k})$. Let $\tilde{W}_{k,l,h}$ be one of the two spaces $\tilde{\tilde{W}}_{k,l,h}$ and $\tilde{\tilde{W}}_{l,k,h}$, achieving the maximum $n_{k,l}$.
For clarity assume that $\tilde{W}_{k,l,h} = \tilde{\tilde{W}}_{k,l,h}$. Let $(\varphi_i), 1 \le i \le n_{k,l}$ be the traces of hat functions of $\tilde{\tilde{W}}_{k,l,h}$ associated to vertices of $\mathcal{T}_{k,h}$ lying on Γ_{kl}, (φ_1 and $\varphi_{n_{k,l}}$ corresponds to the common corners of Ω_k and Ω^l). We define $W_{k,l,h}$ as the vectorial space spanned by $(\varphi_1 + \varphi_2, \varphi_3, ..., \varphi_i, ..., \varphi_{n_{k,l}-2}, \varphi_{n_{k,l}-1} + \varphi_{n_{k,l}})$. $W_{k,l,h}$ is a subspace of $\tilde{W}_{k,l,h}$ of codimension 2.
Let us call W_h the mortar function space :

$$W_h = \prod_{1 \le k < l \le K:\ |\Gamma_{kl}| \neq 0} W_{k,l,h}. \tag{1.6}$$

We are now able to define the discrete space Y_h :

$$Y_h = \left\{ \begin{array}{ll} \mathbf{v}_h = (v_{h,k} \in X_{kh})_k, \quad v_{h,k|\partial\Omega} = 0, & \\ \forall \mu_h \in W_h, \quad \forall 1 \le k < l \le K, & \displaystyle\int_{\Gamma_{kl}} (Tr_k v_{h,k} - Tr_l v_{h,l})\mu_h = 0 \end{array} \right\}. \tag{1.7}$$

The discretized variational formulation is : find $\mathbf{u}_h \in Y_h$ such that

$$\forall \mathbf{v}_h \in Y_h, \quad \sum_{k=1}^{K} \int_{\Omega_k} \nabla u_{h,k} \cdot \nabla v_{h,k} + \eta \sum_{k=1}^{K} \int_{\Omega_k} u_{h,k}\, v_{h,k} = \sum_{k=1}^{K} \int_{\Omega_k} f\, v_{h,k}. \tag{1.8}$$

Clearly the bilinear form in (1.8) is coercive so the discrete problem (1.8) is well posed. This is not so clear for the Laplace operator with Dirichlet conditions. However, even in this case, the coerciveness of the discrete problem can be proved by contradiction , (see [4]).

The error analysis is carried out in [4]. The optimal error estimate is found, inspite of nonconformity.

1.2. Implementation: the saddle point problem.

The aim of this section is to reformulate problem (1.8) into a saddle point problem. Let a_h be the symmetric bilinear form on $X_h \times X_h$:

$$a_h(\mathbf{u}_h, \mathbf{v}_h) = \sum_{k=1}^{K} \int_{\Omega_k} \nabla u_{h,k} \cdot \nabla v_{h,k} \ \mathrm{d}x + \eta \sum_{k=1}^{K} \int_{\Omega_k} u_{h,k}\, v_{h,k} \ \mathrm{d}x. \tag{1.9}$$

We associate to a_h the linear operator A_h such that $(A_h\mathbf{u}_h, \mathbf{v}_h) = a_h(\mathbf{u}_h, \mathbf{v}_h), \quad \forall \mathbf{u}_h, \mathbf{v}_h) \in X_h$. Let b_h be the bilinear form on $X_h \times W_h$

$$b_h(\mathbf{v}_h, \mu_h) = \sum_{1 \le k < l \le K} \int_{\Gamma_{kl}} (Tr_k v_{h,k} - Tr_l v_{h,l})\mu_h. \tag{1.10}$$

We associate to b_h the linear operator B_h from X_h to W_h' such that $(B_h\mathbf{v}_h, \mu_h) = b_h(\mathbf{v}_h, \mu_h), \quad \forall \mu_h \in W_h, \mathbf{v}_h) \in X_h$. Then the space Y_h has the new description :

$$Y_h = \{\mathbf{v}_h \in X_h \text{ such that } \quad B_h\mathbf{v}_h = 0\}. \tag{1.11}$$

Problem (1.8) admits a saddle point formulation of the form : find $(\mathbf{u}_h, \lambda_h) \in X_h \times W_h$ such that

$$\begin{aligned} A_h\mathbf{u}_h + B_h^T\lambda_h &= f_h, \\ B_h\mathbf{u}_h &= 0. \end{aligned} \tag{1.12}$$

We supply X_h with its natural basis of hat functions and W_h with the basis introduced above. Let A and B be the matrices of the operators A_h and B_h in these basis . Let us also call U, Λ and F the vectors corresponding to $\mathbf{u}_h$, λ_h and f_h. Problem (1.12) is equvalent to the following linear system :

$$\begin{pmatrix} A & B^T \\ B & 0 \end{pmatrix} \begin{pmatrix} U \\ \Lambda \end{pmatrix} = \begin{pmatrix} F \\ 0 \end{pmatrix} \tag{1.13}$$

The matrix A is the block diagonal matrix

$$A = \begin{pmatrix} A_1 & & & & & \\ & \cdot & & & & \\ & & \cdot & & & \\ & & & A_k & & \\ & & & & \cdot & \\ & & & & & \cdot \\ & & & & & & A_K \end{pmatrix}$$

each block corresponding to a discrete Neumann problem in subdomain Ω_k, except if $\Omega_k \cap \partial\Omega \neq \emptyset$. Since η is a large positive number, the Neumann problems are well posed.

Eliminating U in system (1.13) leads to the following linear system in Λ :

$$BA^{-1}B^T\Lambda = \Phi = BA^{-1}F, \tag{1.14}$$

and U is given by :

$$U = A^{-1}(F - B^T\Lambda). \tag{1.15}$$

The Uzawa algorithm is in fact the conjugate gradient method applied to system (1.14), whose matrix is positive definite. Such an algorithm allows not to construct effectively the matrices B and B^T, which saves memory.

Remark 1.1 Such a method would not be possible for the Laplace operator, because A may be singular.

1.3. A preconditioned conjugate gradient for a Schur complement method. For all k, $1 \le k \le K$, the finite element space X_{kh} has the following decomposition :

$$X_{kh} = \overset{\circ}{X}_{kh} \oplus Z_{kh}, \tag{1.16}$$

where

$$\overset{\circ}{X}_{kh} = \{ f_h \in X_{kh} \; ; \quad f_h \text{ has value } 0 \text{ on } \partial\Omega_k \} \, . \tag{1.17}$$

For each subdomain Ω_k, we renumber the unknowns as follows : We number first the degrees of freedom of functions of $\overset{\circ}{X}_{kh}$, then those corresponding to Z_{kh}. With this numbering, the matrix A_k is mapped to :

$$\begin{pmatrix} A_{k11} & A_{k12} \\ A_{k12}^T & A_{k22} \end{pmatrix} . \tag{1.18}$$

The matrix A_{k11} corresponds to a Dirichlet problem in Ω_k. Similarly, the vectors U and F in (1.13) are transformed into

$$\begin{pmatrix} U_{11} \\ U_{12} \\ \cdot \\ \cdot \\ U_{k1} \\ U_{k2} \\ \cdot \\ \cdot \\ U_{K1} \\ U_{K2} \end{pmatrix} , \quad \begin{pmatrix} F_{11} \\ F_{12} \\ \cdot \\ \cdot \\ F_{k1} \\ F_{k2} \\ \cdot \\ \cdot \\ F_{K1} \\ F_{K2} \end{pmatrix}$$

Let U_{k1}^0 be the solution of linear system $A_{k11} \, U_{k1}^0 = F_{k1}$, which corresponds to a local Dirichlet problem. Define the block diagonal matrix S, whose k^{th} block is the *Schur complement*

$$S_k = A_{k22} - A_{k12}^T A_{k11}^{-1} A_{k12} \tag{1.19}$$

which can be viewed as the matrix related to the *discrete Steklov Poincaré* operator S_{kh} of subdomain Ω_k.
Then calling V and P the vectors

$$V = \begin{pmatrix} U_{12} \\ \cdot \\ \cdot \\ U_{k2} \\ \cdot \\ \cdot \\ U_{K2} \end{pmatrix} , \quad P = \begin{pmatrix} F_{12} - A_{112}^T U_{11}^0 \\ \cdot \\ \cdot \\ F_{k2} - A_{k12}^T U_{k1}^0 \\ \cdot \\ \cdot \\ F_{K2} - A_{K12}^T U_{K1}^0 \end{pmatrix} ,$$

one checks easily that (V, Λ) solve the linear system :

$$\begin{pmatrix} S & B^T \\ B & 0 \end{pmatrix} \begin{pmatrix} V \\ \Lambda \end{pmatrix} = \begin{pmatrix} P \\ 0 \end{pmatrix} \tag{1.20}.$$

Once this system is solved, U_{k1} is given by :

$$U_{k1} = U_{k1}^0 - A_{k11}^{-1} A_{k12} U_{k2} . \tag{1.21}$$

Following [13], [1], the idea is to solve system (1.20) with a preconditioned conjugate gradient method (PCG) with preconditioner

$$\begin{pmatrix} \tilde{S} & B^T \\ B & 0 \end{pmatrix}, \tag{1.22}$$

where $\tilde{S}$ is a suitably chosen matrix operating on Z_h.
The main feature of this method is the following : if the method is initialized with V_0 such that

$$BV_0 = 0,$$

then, at iteration i, V_i has the same property :

$$\forall i \geq 0, \quad BV_i = 0.$$

In other words, with the special choice (1.22) of preconditioner, the PCG algorithm remains in the kernel of B. The preconditioner is not only used to improve the system's condition number , but also to keep invariant the kernel of B. For now on we shall refer to this method as PCGS (for PCG in Subspace).

The matrix $\tilde{S}$ must satisfy the following requirements :

1) $\tilde{S}$ must be block diagonal with K blocks $\tilde{S}_k$.
2) Each block $\tilde{S}_k$ must be "close" to the discrete Steklov Poincaré matrix S_k.
3) The linear system with matrix $\tilde{S}$ must be easy to solve.
4) Last but not least, the linear system with matrix $B\tilde{S}^{-1}B^T$ must be easy to solve.

Remark 1.2 As opposed to the Uzawa methods described above, this Schur complement method can be applied in a straightforward manner to Laplace operator because it is based on solving Dirichlet problems (instead of Neumann) in each subdomain. Such a preconditioned conjugate gradient method for the Laplace operator is described in [1].

2 PRECONDITIONERS BASED ON A CONTINUOUS ANALYSIS.

The requirements for $\tilde{S}$ stated in §1.3 led us to focus on the following class of matrices : $\tilde{S}$ is block diagonal with K blocks $\tilde{S}_k$. The block $\tilde{S}_k$ corresponds to the finite element discretization of

$$\alpha_k(s) - \frac{d}{ds}\beta_k(s)\frac{d}{ds}, \tag{2.1}$$

where s is the curvilinear abcissa on $\partial\Omega_k$, α_k and β_k are two positive functions on $\partial\Omega_k$, to be determined. In the following, we shall see that, if the mesh is uniform in Ω_k, these function can be taken edgewise constant on $\partial\Omega_k$.
It is not clear a priori why a linear system with matrix $B\tilde{S}^{-1}B^T$ should be easy to solve : it is actually (at the cost of a rather large amount of programming work though) and we refer to [1] for the algorithm.
In this section, we shall show how to determine these constants by a continuous analysis, *i.e.* we shall try to approximate the continuous Steklov Poincaré operator $\mathcal{S}$ (truncated in Fourier space) by $\tilde{\mathcal{S}}$ in the class (2.1). We shall see later that studying directly the discrete Steklov Poincaré operator yields a better preconditioner, especially when the mesh exhibits large aspect ratios. However, the continuous analysis is simpler than the discrete one, and yet contains the same technical arguments.

2.1 A model case.

We are going to focus on a model problem, with two subdomains separated by a single edge Γ. The simplest case is that of an an infinite strip Ω separated into two semi-infinite subdomains Ω_1 and Ω_2.

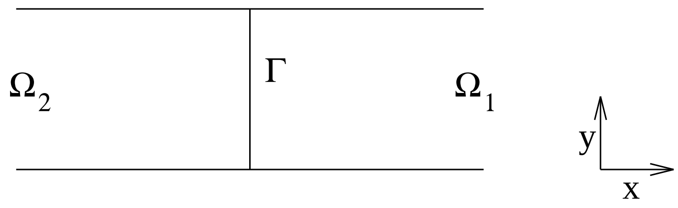

Figure 2.1 : The model geometry .

The system of coordinates can be chosen such that Γ is the segment $\{0\} \times [0, d]$.

In this special case, we have to approximate one Steklov Poincaré operator per subdomain. For symmetry reasons, we are going to focus on subdomain Ω_1.

Let us study the Steklov Poincaré operator related to the following boundary value problem :

$$\begin{aligned}
&-\Delta u + \eta u = 0 \quad \text{in } \Omega_1,\\
&u = 0 \quad \text{on } \partial\Omega_1 \backslash \Gamma,\\
&u = u_{|\Gamma} \quad \text{on } \Gamma.
\end{aligned} \tag{2.2}$$

The Steklov Poincaré $\mathcal{S}$ maps $u_{|\Gamma}$ to $\frac{\partial u}{\partial n}$ with u solution of (2.2). One can check that $\mathcal{S}$ is diagonal in the following Fourier basis :

$$\sin(n\frac{\pi y}{d}).$$

Indeed,

$$\mathcal{S}\sin(n\frac{\pi y}{d}) = \sqrt{\eta + \left(\frac{n\pi}{d}\right)^2}\sin(n\frac{\pi y}{d}).$$

At this point, we should remember that we are dealing with finite element discretisation, and that the number of Fourier modes effectively taken into account is

$$N \approx \frac{d}{\pi h},$$

where h is the mesh step in the y direction. Let us call H_N the vectorial space spanned by $\left(\sin(n\frac{\pi y}{d})\right)_{0\leq n\leq N}$. The Steklov Poincaré operator as well as any derivation operator keep H_N invariant. Our goal is to approximate $\mathcal{S}$ on H_N with a local, symmetric and positive operator $\tilde{\mathcal{S}}(\beta)$ in the class :

$$\tilde{\mathcal{S}}(\beta) = \sqrt{\eta}(I - \beta\Delta_{|\Gamma}), \tag{2.3}$$

where β is a parameter to determine and $\Delta_{|\Gamma}$ is the Laplace-Beltrami operator on Γ.

The most naive idea for doing so may be to take the low frequency approximation of the Steklov Poincaré operator *i.e*, to carry out a second order Taylor expansion of its symbol at the origin

$$\sqrt{\eta + k^2} = \sqrt{\eta} + \frac{k^2}{2\sqrt{\eta}} + O(k^4).$$

This leads to choosing $\tilde{\mathcal{S}}(\beta)$ as

$$\sqrt{\eta} - \frac{1}{2\sqrt{\eta}}\Delta_{|\Gamma},$$

which is a very good approximation only for the lowest freqencies. With this choice, the condition number of $\tilde{\mathcal{S}}^{-1}(\beta)\mathcal{S}$ on H_N, obtained after an easy calculation, is of order $O((h^2\eta)^{-\frac{1}{2}})$. Since the condition number of $\mathcal{S}$ itself has the same asymptotic behaviour, this naive choice of $\tilde{\mathcal{S}}(\beta)$ is clearly not optimal.

A less naive goal will be to minimize the condition number of $\tilde{\mathcal{S}}^{-1}(\beta)\mathcal{S}$ on H_N, for $\tilde{\mathcal{S}}(\beta)$ in the class (2.3). We have the following proposition :

Proposition 2.1 *Assume $h^2\eta \ll 1$, (the mesh can catch boundary layer effects), then the minimum condition number of $\tilde{\mathcal{S}}^{-1}(\beta)\mathcal{S}$ on H_N, for $\tilde{\mathcal{S}}(\beta)$ in the class (2.3) is a $O((h^2\eta)^{-\frac{1}{4}})$. The operator*

$$\tilde{\mathcal{S}}(\frac{h}{\sqrt{\eta}}) = \sqrt{\eta} - h\Delta_{|\Gamma} \tag{2.4}$$

yields a condition number with such an asymptotic behaviour.

Proof Of course the operator $\tilde{\mathcal{S}}(\beta)$ is diagonal in the Fourier basis :

$$\tilde{\mathcal{S}}(\beta)\sin(n\frac{\pi y}{d}) = \sqrt{\eta}\left(1 + \beta\left(\frac{n\pi}{d}\right)^2\right)\sin(n\frac{\pi y}{d}) \tag{2.5}$$

Calling f and g_β the real functions :

$$\begin{aligned} f(t) &= \sqrt{1 + \frac{t}{\eta}}, \\ g_\beta(t) &= 1 + \beta t \end{aligned} \tag{2.6}$$

minimizing the condition number of $\tilde{\mathcal{S}}^{-1}(\beta)\mathcal{S}$ restricted to the space spanned by the N first Fourier modes leads to the following minimization problem : find β minimizing

$$\frac{\displaystyle\max_{0\le n\le N} \frac{g_\beta}{f}\left(\left(\frac{n\pi}{d}\right)^2\right)}{\displaystyle\min_{0\le n\le N} \frac{g_\beta}{f}\left(\left(\frac{n\pi}{d}\right)^2\right)}. \tag{2.7}$$

This discrete problem being too difficult, we replace it by the continuous one : find β minimizing the non differentiable function $c(\beta)$:

$$c(\beta) = \frac{\displaystyle\max_{0\le t\le \frac{1}{h^2}} \frac{g_\beta}{f}}{\displaystyle\min_{0\le t\le \frac{1}{h^2}} \frac{g_\beta}{f}}. \tag{2.8}$$

This minimization can be done almost entirely by geometrical arguments. The following analysis will also be used in the study of the discrete Steklov Poincaré operator in section 3.
It is clear that $\forall\beta > 0$, the graphs of f and g_β intersect at the origin. Moreover, the graphs can intersect at at most 2 points. Indeed, we can make out three cases :
Case 1 : $\beta > \frac{1}{2\eta}$, then $\frac{g_\beta}{f}(t) > 1, \forall t > 0$.
Case 2 : $\beta < h^2\left(\sqrt{1+\frac{1}{h^2\eta}} - 1\right)$, then $\frac{g_\beta}{f}(t) < 1, \forall t \le \frac{1}{h^2}$.
Case 3 : $h^2\left(\sqrt{1+\frac{1}{h^2\eta}} - 1\right) \le \beta \le \frac{1}{2\eta}$ then the curves of g_β and f intersect at zero and another point t_c with $0 \le t_c \le \frac{1}{h^2}$.

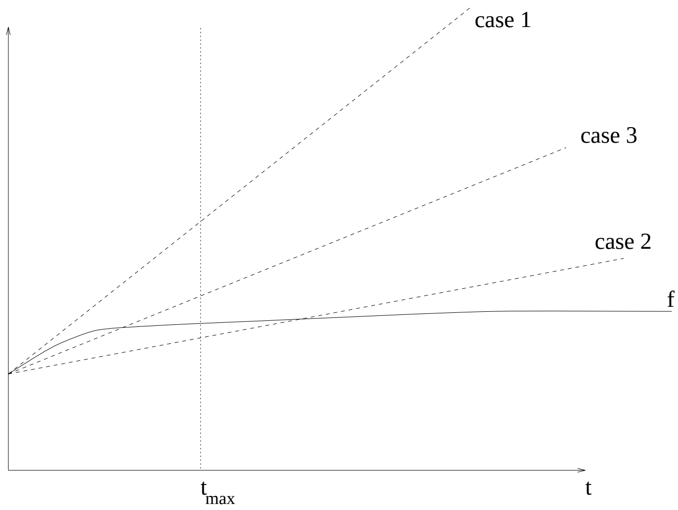

Figure 2.2 : three different cases

• **Case 1** $\beta > \frac{1}{2\eta}$ then $\frac{g_\beta}{f}(t) > 1, \forall t > 0$. Then $c(\beta) = \frac{g_\beta}{f}(\frac{1}{h^2})$ is clearly an increasing function of β. Hence the minimum of $c(\beta)$ is not reached in this interval.

• **Case 2** $\beta < h^2\left(\sqrt{1+\frac{1}{h^2\eta}} - 1\right)$, then $\frac{g_\beta}{f}(t) < 1, \forall t \le \frac{1}{h^2}$. Then $c(\beta) = \displaystyle\max_{0\le t\le \frac{1}{h^2}} \frac{f}{g_\beta}$ is a decreasing function function of β. Hence the minimum of $c(\beta)$ is not reached in this interval.

Therefore, the minimum of $c(\beta)$ is reached in the interval $[h^2\left(\sqrt{1+\frac{1}{h^2\eta}}-1\right), \frac{1}{2\eta}]$. In this case, the graph of g_β cuts another time the graph of f at t_c with $0 \leq t_c \leq \frac{1}{h^2}$.

• **Case 3** $\beta \in [h^2\left(\sqrt{1+\frac{1}{h^2\eta}}-1\right), \frac{1}{2\eta}]$. It can be shown that the derivative of $\frac{g_\beta}{f}$ vanishes only once, at $t_\circ$ in the interval $[0, t_c]$ and is positive for $t > t_c$. Therefore the maximum of $\frac{g_\beta}{f}$ is greater than 1 and is reached at $\frac{1}{h^2}$, and the minimum of $\frac{g_\beta}{f}$ is smaller than 1 and is reached at $t_\circ < t_c$. Instead of $c(\beta)$, we consider

$$\begin{aligned}\log(c(\beta)) &= \underset{0\leq t\leq \frac{1}{h^2}}{max} \log\left(\frac{g_\beta}{f}\right) - \underset{0\leq t\leq \frac{1}{h^2}}{min} \log\left(\frac{g_\beta}{f}\right) \\ &= \log\left(\frac{g_\beta}{f}(\frac{1}{h^2})\right) - \log\left(\frac{g_\beta}{f}(t_\circ)\right)\end{aligned}$$

Let us show that this quantity is an increasing function of β : Let $\delta\beta$ be a small positive variation of β, then

$$\log\left(\frac{g_{\beta+\delta\beta}}{f}\right)(t) = \log\left(\frac{g_\beta}{f}\right)(t) + \log\left(\frac{g_{\beta+\delta\beta}}{g_\beta}\right)(t).$$

In particular,

$$\log\left(\frac{g_{\beta+\delta\beta}}{f}\right)(t_\circ) \leq \log\left(\frac{g_\beta}{f}\right)(t_\circ) + \log\left(\frac{g_{\beta+\delta\beta}}{g_\beta}\right)(\frac{1}{h^2}),$$

because $\frac{g_{\beta+\delta\beta}}{g_\beta}$ is clearly an increasing function if $\delta\beta$ is positive. Taking the minimum of $\log\left(\frac{g_{\beta+\delta\beta}}{f}\right)$, we obtain that

$$\log\left(\frac{g_{\beta+\delta\beta}}{f}\right)(t_\circ+\delta t_\circ) - \log\left(\frac{g_\beta}{f}\right)(t_\circ) < \log\left(\frac{g_{\beta+\delta\beta}}{g_\beta}\right)(\frac{1}{h^2}).$$

Hence, the variation of the minimum of $\log\left(\frac{g_\beta}{f}\right)$ is smaller than the variation of its maximum. Therefore, $\log(c(\beta))$ is an increasing function of β. Its minimum is reached at $h^2\left(\sqrt{1+\frac{1}{h^2\eta}}-1\right)$. If $h^2\eta \ll 1$, which is a likely hypothesis if the mesh is expected to catch the boundary layer effects, the optimal parameter β_{opt} is equivalent to $\frac{h}{\sqrt{\eta}}$, and the optimal operator $\tilde{\mathcal{S}}(\beta_{opt})$ is $\sqrt{\eta} - h\Delta_\Gamma$. Now, to estimate the condition number, one has to compute $t_\circ$ for $\beta = \frac{h}{\sqrt{\eta}}$. Easy calculations show that $t_\circ \approx \frac{\sqrt{\eta}}{h}$ and that the condition number is of order $O(h^2\eta)^{-\frac{1}{4}})$.
Finally, it is obvious that the minimum of the discrete problem is smaller than that of the continuous one. □

Remark 2.1 Note that the last choice of $\tilde{\mathcal{S}}(\beta)$ yields a good approximation of $\mathcal{S}$ for the lowest and highest frequencies permitted by the mesh. For intermediate frequencies, this approximation is not as good.

On proving proposition 2.1, we have in fact proved a general lemma which will be useful later on :

Lemma 2.1 *Let f be a C^1 concave function on $[0,T]$. Let $(g_\beta)_{\beta\in[\beta_\circ,\beta_1]}$ be a family of increasing C^1 convex functions on $[0,T]$ such that :*
1) $\forall t \in [0,T]$, *$g_\beta(t)$ is a strictly increasing function of β.*

2) $g_\beta(0) = f(0), \quad \forall \beta \in [\beta_\circ, \beta_1]$.
3) *There exists a one to one decreasing function* $\beta \to t_c(\beta)$ *from* $[\beta_\circ, \beta_1]$ *onto* $[0, T]$ *such that :*
$g_\beta(t) \leq f(t)$ *for* $0 \leq t \leq t_c(\beta)$.
$g_\beta(t) \geq f(t)$ *for* $t_c(\beta) \leq t \leq T$.

Then the function

$$c(\beta) = \frac{\displaystyle\max_{0 \leq t \leq \frac{1}{T}} \frac{g_\beta}{f}}{\displaystyle\min_{0 \leq t \leq \frac{1}{T}} \frac{g_\beta}{f}}$$

is an increasing function of β.

2.2 The general case.

Let us consider now a general domain decomposition of Ω into non overlapping subdomains $(\Omega_k)_{1 \leq k \leq K}$ as described in section 1. We assume that $\forall\ 1 \leq k \leq K$, the mesh $\mathcal{T}_{kh}$ of subdomain Ω_k is uniformly regular with a size h independant of k. The Steklov Poincaré operator S_h is a block diagonal operator with K blocks, the k^{th} block being the Steklov Poincaré operator S_{kh} of subdomain Ω_k : for all $u_{kh},\ v_{kh} \in Z_{kh}$,

$$(S_{kh} u_{kh}, v_{kh}) = \int_{\Omega_k} \nabla \tilde{u}_{kh} \cdot \nabla \bar{v}_{kh} + \eta \int_{\Omega_k} \tilde{u}_{kh} \bar{v}_{kh}, \tag{2.9}$$

where $\bar{v}_{kh}$ is any lifting of v_{kh} in X_{kh}, and where $\tilde{u}_{kh}$ is the solution of the following problem

$$\tilde{u}_{kh} = u_{kh} \quad \text{on } \partial\Omega_k,$$

$$\forall w_{kh} \in X_{kh} \text{ such that } w_{kh} = 0 \text{ on } \partial\Omega_k, \qquad \int_{\Omega_k} \nabla \tilde{u}_{kh} \cdot \nabla w_{kh} + \eta \int_{\Omega_k} \tilde{u}_{kh} w_{kh} = 0.$$

For all $1 \leq k \leq K$, let us introduce the operator $\tilde{S}_{kh} : Z_{kh} \to Z_{kh}$:

$$\left(\tilde{S}_{kh} u_{kh}, v_{kh}\right) = h \int_{\partial\Omega_k} \frac{\partial u_{kh}}{\partial s} \frac{\partial v_{kh}}{\partial s} + \sqrt{\eta} \int_{\partial\Omega_k} u_{kh} v_{kh}, \tag{2.10}$$

and $\tilde{S}_h$ the block diagonal operator with K blocks, the k^{th} block being $\tilde{S}_{kh}$. Note that $\tilde{S}_h$ is the discretized version of operator $\tilde{\mathcal{S}}(\beta_{opt})$ introduced in (2.4). We have the following result :

Proposition 2.2 *There exists constants* c_1 *and* c_2 *independant of* h *and* η *such that, for all* h *and* η *with* $\eta h^2 < 1$,

$$\forall u_{kh} \in Z_{kh}, \qquad c_1 \leq \frac{(S_{kh} u_{kh}, u_{kh})}{\left(\tilde{S}_{kh} u_{kh}, u_{kh}\right)} \leq \frac{c_2}{(\eta h^2)^{\frac{1}{4}}} \tag{2.11}$$

Proof Calling $\Omega_{k\eta}$ the dilated domain

$$\Omega_{k\eta} = \sqrt{\eta}\, \Omega_k, \tag{2.12}$$

a change of variables yields that $\forall u \in H^1(\Omega_k)$,

$$\int_{\Omega_k} |\nabla u|^2 + \eta \int_{\Omega_k} u^2 = \int_{\Omega_{k\eta}} |\nabla v|^2 + \int_{\Omega_{k\eta}} v^2, \tag{2.13}$$

where $v(x) = u(\frac{x}{\sqrt{\eta}})$.
Let us call $X_{k\sqrt{\eta}h}$ the finite element space on $\Omega_{k\eta}$ defined by

$$X_{k\sqrt{\eta}h} = \left\{ w_{kh}(\frac{x}{\sqrt{\eta}}) \quad ; \quad w_{kh} \in X_{kh} \right\}.$$

We deduce from (2.13) that, with the notations above, $\tilde{v}_{kh}(x) = \tilde{u}_{kh}(\frac{x}{\sqrt{\eta}})$ is the solution of the finite element problem :

$$\tilde{v}_{kh} = v_{kh} \quad \text{on } \partial\Omega_{k\eta},$$

$$\forall w_{kh} \in X_{k\sqrt{\eta}h} \text{ such that } w_{kh} = 0 \text{ on } \partial\Omega_{k\eta}, \qquad \int_{\Omega_{k\eta}} \nabla\tilde{v}_{kh} \cdot \nabla w_{kh} + \int_{\Omega_{k\eta}} \tilde{v}_{kh} w_{kh} = 0,$$

where $v_{kh}(x) = u_{kh}(\frac{x}{\sqrt{\eta}})$. Thus, following [16],[5], and [7], it is possible to prove that

$$c_1 ||v_{kh}||^2_{\frac{1}{2},\partial\Omega_{k\eta}} \le (S_{kh}u_{kh}, u_{kh}) \le c_2 ||v_{kh}||^2_{\frac{1}{2},\partial\Omega_{k\eta}},$$

with c_1 and c_2 independant of η and h. Since $H^{\frac{1}{2}}(\partial\Omega_{k\eta})$ is the interpolated space beetween $H^1(\partial\Omega_{k\eta})$ and $L^2(\partial\Omega_{k\eta})$, we have

$$c_1 ||v_{kh}||^2_{\frac{1}{2},\partial\Omega_{k\eta}} \le (S_{kh}u_{kh}, u_{kh}) \le c_2 ||v_{kh}||_{1,\partial\Omega_{k\eta}} ||v_{kh}||_{0,\partial\Omega_{k\eta}}.$$

Using the obvious estimate $||v_{kh}||_{0,\partial\Omega_{k\eta}} \le ||v_{kh}||_{\frac{1}{2},\partial\Omega_{k\eta}}$ and the inverse inequality for finite elements on the other hand :

$$||\nabla v_{kh}||^2_{0,\partial\Omega_{k\eta}} \le C \frac{1}{\sqrt{\eta}h} ||v_{kh}||^2_{\frac{1}{2},\partial\Omega_{k\eta}},$$

we obtain the following estimate :

$$c_1 \left(\sqrt{\eta}h ||\nabla v_{kh}||^2_{0,\partial\Omega_{k\eta}} + ||v_{kh}||^2_{0,\partial\Omega_{k\eta}} \right) \le (S_{kh}u_{kh}, u_{kh}) \le c_2 ||v_{kh}||_{1,\partial\Omega_{k\eta}} ||v_{kh}||_{0,\partial\Omega_{k\eta}}.$$

Performing the inverse change of variable as above, we obtain :

$$c_1 \left(h ||\nabla v_{kh}||^2_{0,\partial\Omega_k} + \sqrt{\eta} ||v_{kh}||^2_{0,\partial\Omega_{k\eta}} \right) \le (S_{kh}u_{kh}, u_{kh})$$
$$\le c_2 \left(\frac{1}{\sqrt{\eta}} ||\nabla u_{kh}||^2_{0,\partial\Omega_k} + \sqrt{\eta} ||u_{kh}||^2_{0,\partial\Omega_k} \right)^{\frac{1}{2}} (\eta)^{\frac{1}{4}} ||u_{kh}||_{0,\partial\Omega_k}.$$

Calling t the ratio

$$t = \frac{||\nabla u_{kh}||^2_{0,\partial\Omega_k}}{||u_{kh}||^2_{0,\partial\Omega_k}},$$

we have

$$c_1 \left(ht + \sqrt{\eta} \right) ||u_{kh}||^2_{0,\partial\Omega_k} \le (S_{kh}u_{kh}, u_{kh}) \le c_2 \sqrt{t + \eta}\, ||u_{kh}||^2_{0,\partial\Omega_k},$$

which implies :

$$c_1 \le \frac{(S_{kh}u_{kh}, u_{kh})}{\left(\tilde{S}_{kh}u_{kh}, u_{kh} \right)} \le c_2 \frac{\sqrt{t+\eta}}{ht + \sqrt{\eta}}. \tag{2.14}$$

From the inverse inequality for finite elements, we have the following bounds on t :

$$0 \le t \le \frac{1}{h^2}. \tag{2.15}$$

With (2.14) and (2.15) the result follows from those of proposition 2.1. □

3 PRECONDITIONERS BASED ON A DISCRETE ANALYSIS .

The preconditioners derived in section 2 were meant to approach the continuous Steklov Poincaré operator $\mathcal{S}$ for the frequencies permitted by the mesh. It is sensible that if the mesh steps h_x and h_y are small enough *i.e.*

$$h_x^2\eta \ll 1, \quad h_y^2\eta \ll 1, \tag{3.1}$$

the discrete Steklov Poincaré operator S_h is close enough to $\mathcal{S}$ so that the previous continuous analysis will supply a good preconditioner. However, in many practical applications, the two mesh steps h_x and h_y need not satisfy the inequalities (3.1). Indeed, if we consider a high Reynolds number flow around a body, the viscous effects are negligible far away from the body and the wake of the flow. In this region, the mesh need not be fine, hence

$$h_x^2\eta \gg 1, \quad h_y^2\eta \gg 1.$$

Another example is that of a laminar boundary layer : in such a region, the mesh must be fine only in the direction normal to the wall; for instance, for a wall $y = constant$

$$h_x^2\eta \gg 1, \quad h_y^2\eta \ll 1.$$

In these cases, it is very likely that the continuous analysis above will not supply a good preconditioner. Therefore, it seems useful to carry out the whole discrete analysis at least in the simple case described on figure 2.1. To do it, we need first to compute the Steklov Poincaré operator S_h corresponding to the discretization.

3.1 The discrete Steklov Poincaré operator in a model case

The chosen discretization is that of Q_1 finite element method. In the following model case, the Steklov Poincaré operator can be computed by hand :

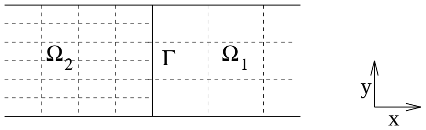

Figure 3.1 : 2 subdomains with non matching grids

Note that the grids are uniform in both subdomains. As above, we are going to focus on subdomain Ω_1. The quadrangulation is made of $N+1$ horizontal lines and an infinite number of vertical segments. The intersection beetween the i^{th} vertical segment and the j^{th} horizontal line is the point $P_{i,j}$. As in section 1, we call X_{1h} the space of Q_1 finite element vanishing on $\partial\Omega_1\backslash\Gamma$. We denote by $e_{i,j}$ the finite element function taking the value 1 at $P_{i,j}$ and 0 at all the other vertices of the quadrangulation. The discrete Steklov Poincaré operator S_h, already mentioned in (2.9), is defined by :

$$\forall l, m \in \{1, N-1\}, \quad \langle S_h e_{0,l}\,,\, e_{0,m}\rangle = \int_{\Omega_1} \nabla v_{0,l}\cdot\nabla e_{0,m} + \eta v_{0,l}e_{0,m},$$

where $v_{0,l} \in X_{1h}$ is defined by :

$$\begin{aligned} &v_{0,l} = e_{0,l} \quad \text{on } \Gamma, \\ &\forall z \in X_{1h} \text{ with } z = 0 \text{ on } \Gamma, \quad \int_{\Omega_1} \nabla v_{0,l}\cdot\nabla z\eta v_{0,l}z = 0. \end{aligned} \tag{3.2}$$

Instead of studying S_h we are going to compute first S_h^{-1}, which leads to considering the discretised problem corresponding to

$$\begin{aligned}
&-\Delta u + \eta u = 0 \quad \text{ in } \Omega_1, \\
&u = 0 \quad \text{ on } \partial\Omega_1 \backslash \Gamma, \\
&\frac{\partial u}{\partial n} \quad \text{ given on } \Gamma.
\end{aligned} \tag{3.3}$$

Calling $u_{i,j}$ the degree of freedom corresponding to the basis function $e_{i,j}$, the vector U defined by $U_{j+i(N+1)} = u_{i,j}$ satisfies

$$AU = G, \tag{3.4}$$

where the matrix A can be expressed in terms of four coefficients $A_{00}, A_{01}, A_{10}, A_{11}$ (see (3.6),(3.7),(3.8) below) and where the vector G is defined by $G_0 = 0, \quad G_j = g_j, \ \forall j \in \{1,..N-1\}, \quad G_j = 0, \ \forall j \geq N$. We shall denote by S the matrix of S_h in the basis $(e_{0,l})_{l\in\{1,N-1\}}$. It is defined by

$$S^{-1}(g_j)_{j\in\{1,..N-1\}} = (u_{0,j})_{j\in\{1,..N-1\}}. \tag{3.5}$$

As for the continuous case, we introduce a Fourier basis $(F^n)_{n\in\{1,..N-1\}}$ of R^{N-1}, namely

$$F^n = \left(\sin(\frac{n\pi}{N}j)\right)_{j\in\{1,..N-1\}}.$$

It will turn out that S is diagonal in the basis $(F^n)_{n\in\{1,..N-1\}}$. Let us compute $S^{-1}F^n$, *i.e.* solve the following linear system :

$$\forall i > 1, \forall 1 \leq j \leq N-1, \sum_{\beta=-1}^{1} A_{0,|\beta|} u^n_{i,j+\beta} + A_{1,|\beta|}(u^n_{i+1,j+\beta} + u^n_{i-1,j+\beta}) = 0, \tag{3.6}$$

$$\forall 1 \leq j \leq N-1, \sum_{\beta=-1}^{1} \frac{1}{2} A_{0,|\beta|} u^n_{0,j+\beta} + A_{1,|\beta|} u^n_{1,j+\beta} = \sin(\frac{n\pi}{N}j), \tag{3.7}$$

$$\forall i \geq 0, u^n_{i,0} = u^n_{i,N} = 0. \tag{3.8}$$

We look for the solution in the form :

$$u^n_{i,j} = \alpha_n \sin(\frac{n\pi}{N}j) e^{-z_n i}, \tag{3.9}$$

where α_n and z_n are two constants to be determined. The constant z_n is fixed by equation (3.6). Indeed, (3.6) becomes :

$$\sum_{\beta=-1}^{1} A_{1,|\beta|} \sin(\frac{n\pi}{N}(j+\beta)) + A_{0,|\beta|} \sin(\frac{n\pi}{N}(j+\beta)) e^{-z_n} + A_{1,|\beta|} \sin(\frac{n\pi}{N}(j+\beta)) e^{-2z_n} = 0. \tag{3.10}$$

Calling S_0^n and S_1^n the quantities

$$S_0^n = \sum_{\beta=-1}^{1} A_{0,|\beta|} \cos(\frac{n\pi}{N}\beta), \quad S_1^n = \sum_{\beta=-1}^{1} A_{1,|\beta|} \cos(\frac{n\pi}{N}\beta), \tag{3.11}$$

(3.10) implies that e^{-z_n} is a solution of the second order equation :

$$S_1^n + e^{-z_n} S_0^n + e^{-2z_n} S_1^n = 0. \tag{3.12}$$

Now equation (3.7) yields :

$$\alpha_n = \frac{2}{S_0^n + 2S_1^n e^{-z_n}}. \tag{3.13}$$

Eliminating e^{-z_n} beetween (3.12) and (3.13) yields :

$$\alpha_n = \frac{2}{\sqrt{{S_0^n}^2 - 4{S_1^n}^2}}.$$

Therefore, α_n is the n^{th} eigenvalue of S^{-1}, and corresponds to eigenvector F^n.
Note that the stiffness matrix L related to the discrete Laplace operator Δ_h on Γ is diagonal in the same Fourier basis :

$$LF^n = \frac{l_n}{h_y} F^n, \qquad \text{with} \qquad l_n = 2 - 2\cos(\frac{n\pi}{N}). \tag{3.14}$$

In the following, it will be convenient to use $\mathcal{L} = h_y L$ the positive definite matrix defined by

$$\mathcal{L} = h_y L, \qquad \mathcal{L}F^n = l_n F^n. \tag{3.15}$$

Remark 3.1 Note that the eigenvalues of $\mathcal{L}$ lie in the interval $]0,4[$.

We wish to express the eigenvalue α^n in terms of l_n and the parameters ηh_x^2 and ηh_y^2. Easy algebra indicates that

$$\begin{aligned} A_{0,0} &= \tfrac{4}{3}(\tfrac{h_x}{h_y} + \tfrac{h_y}{h_x}) + \tfrac{4}{9}\eta h_x h_y, & A_{0,1} &= \tfrac{1}{3}(-2\tfrac{h_x}{h_y} + \tfrac{h_y}{h_x}) + \tfrac{1}{9}\eta h_x h_y, \\ A_{1,0} &= \tfrac{1}{3}(\tfrac{h_x}{h_y} - 2\tfrac{h_y}{h_x}) + \tfrac{1}{9}\eta h_x h_y, & A_{1,1} &= -\tfrac{1}{6}(\tfrac{h_x}{h_y} + \tfrac{h_y}{h_x}) + \tfrac{1}{36}\eta h_x h_y. \end{aligned}$$

Then calculations lead to

$$\begin{aligned} S_0^n &= 2\frac{h_y}{h_x} - \frac{1}{3}(\frac{h_y}{h_x} - 2\frac{h_x}{h_y})l_n + \eta h_x h_y(\frac{2}{3} - \frac{1}{9}l_n), \\ S_1^n &= -\frac{h_y}{h_x} + \frac{1}{6}(\frac{h_y}{h_x} + \frac{h_x}{h_y})l_n + \eta h_x h_y(\frac{1}{6} - \frac{1}{36}l_n). \end{aligned}$$

Thus the eigenvalue α_n reads :

$$\alpha_n = \frac{(3(\eta h_x^2 + 12))^{-\frac{1}{2}}}{h_y} \frac{1}{f(l_n)}, \tag{3.16}$$

where

$$f(l_n) = \left(1 + l_n(-\frac{1}{3} + \frac{2}{\eta h_y^2}\frac{\eta h_x^2 + 6}{\eta h_x^2 + 12}) + {l_n}^2(\frac{1}{36} - \frac{1}{3\eta h_y^2}\frac{\eta h_x^2 + 6}{\eta h_x^2 + 12} + \frac{\eta h_x^2}{\eta^2 h_y^4(\eta h_x^2 + 12)})\right)^{\frac{1}{2}}. \tag{3.17}$$

It can be checked that $f(l_n)$ is well defined for $0 \leq l_n \leq 4$, and that it is always a concave function of l_n. Therefore, in terms of matrix $\mathcal{L}$ (see 3.15),

$$S = h_y \sqrt{3(\eta h_x^2 + 12)} f(\mathcal{L}). \tag{3.18}$$

Remark 3.2 In (3.17), the relevant parameters are ηh_x^2 and ηh_y^2 : These quantities measure how the finite element approximation will take into account the viscous effects in each direction of the grid.

Remark 3.3 The discrete Steklov Poincaré operator can also be thoroughly computed in the case of an oblique grid with periodic boundary conditions :

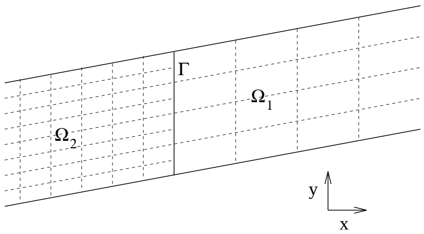

Figure 3.2 : Oblique grids

In this case, the matrix A is totally determined by 5 coefficients : $A_{0,0}, A_{0,1}, A_{1,0}, A_{1,1}, A_{1,-1}$. Then the operator S can be written :

$$S = \begin{pmatrix} (A_{0,0} + 2A_{0,1})2 - 4(A_{1,-1} + A_{1,0} + A_{1,1})^2 + 4\mathcal{L}'(A_{1,0}(A_{1,-1} + A_{1,1}) + 4A_{1,-1}A_{1,1}) \\ + \mathcal{L}'^2(A_{0,1}^2 - 4A_{1,-1}A_{1,1}) \end{pmatrix}^{\frac{1}{2}},$$

where $\mathcal{L}'$ is the diagonal operator with eigenvalues $2 - 2\cos(\frac{2\pi n}{N})$ in the Fourier basis $F'^n = (e^{i\frac{2\pi n}{N}j})_{0 \leq j \leq N}$. □

Remark 3.4 It is also possible to study explicitely the discrete Steklov operator in the following model case. Subdomain Ω_1' is the rectangle $\Omega_1 \cap \{-\infty < x < D\}$, where Ω_1 is defined in Figure 3.1, and homogeneous Dirichlet conditions are imposed on horizontal sides. As above, it is possible to define the restriction of the discrete Steklov-Poincaré matrix to side Γ, namely S_h'. It is possible to approach S_h' by S_h defined by (3.2). Indeed, it can be shown that the error beetween these two operators behaves like $e^{-z_n \frac{D}{h_x}}$ where z_n is given by (3.12). This error is estimated by

Lemma 3.1
Assume $\min(h_x, h_y) < \sqrt{\frac{6}{\eta}}$ *and let* $C_\circ = -\log(5(1 - \sqrt{1 - \frac{1}{25}})) \sim 2.29$ *then,*

1 $h_x > \sqrt{\frac{6}{\eta}} \Rightarrow e^{-z_n \frac{D}{h_x}} \leq e^{\frac{-D}{h_x} C_\circ}$.

2 $h_x < \sqrt{\frac{6}{\eta}} \Rightarrow \exists c > 0$ *independant of* h_x, h_y *and* $\sqrt{\eta}$, *such that* $e^{-z_n \frac{D}{h_x}} \leq e^{-\sqrt{\eta} D c}$

proof see the appendix. □

As in the continuous case, the discrete Steklov Poincaré operator is not local, because it can be written as the square root of a positive definite matrix corresponding to a local operator. In next paragraph, we are going to seek local approximations of S.

3.2 Preconditioners

As in the continuous analysis, we are going to seek $\tilde{S}$ in the form : $\tilde{S} = c_0 M - c_1 L$, where L is the stiffness matrix (discretised Laplace operator) on Γ, and M is the mass matrix on Γ. Note that the mass matrix can be written :

$$M = h_y(I - \frac{1}{6}\mathcal{L}). \tag{3.19}$$

The strategy here will also consist in trying to minimize the condition number of $\tilde{S}^{-1}S$.

Thanks to (3.15),(3.19), searching $\tilde{S}(\beta)$ in the form :

$$\tilde{S}(\beta) = \sqrt{3(\eta h_x^2 + 12)}h_y(I + \beta\mathcal{L}) = \sqrt{3(\eta h_x^2 + 12)}(M + (\beta + \frac{1}{6})h_y^2 L) \tag{3.20}$$

is equivalent to finding $\beta \geq -\frac{h_y}{6}$ minimizing :

$$\frac{\underset{1\leq n\leq N-1}{max} \frac{g_\beta}{f}(l_n)}{\underset{1\leq n\leq N-1}{min} \frac{g_\beta}{f}(l_n)}, \tag{3.21}$$

where (l_n) is given by (3.14), f is given by (3.17), and where

$$g_\beta(l_n) = 1 + \beta l_n. \tag{3.22}$$

It is also obvious that the minimum of this discrete problem is smaller than that of the continuous one : find $\beta_{opt} \geq -\frac{h_y}{6}$ minimizing $c(\beta)$:

$$c(\beta) = \frac{\underset{0\leq t\leq 4}{max} \frac{g_\beta}{f}(t)}{\underset{0\leq t\leq 4}{min} \frac{g_\beta}{f}(t)}. \tag{3.23}$$

For simplicity, we shall limit ourselves to the case

$$\eta h_y^2 \leq \frac{3}{2}.$$

For these values of h_y, (in fact, it suffices that $\eta h_y^2 \leq 3$), the derivative of f at $t = 0$ is positive for all h_x. For larger values of h_y, the condition number of S is bounded by a constant independantly of h_y and h_x, so there is not really a point in preconditioning for the model case. For a general domain decomposition with more than one interface, it is enough to precondition by the 0^{th} order approximation of S restricted to edge Γ, namely $\sqrt{3(\eta h_x^2 + 12)}M_{|\Gamma}$.

The following proposition is a corollary of lemma 2.1.

Proposition 3.1 *Assume $h_y^2\eta \leq \frac{3}{2}$, then $\beta_{opt} \geq -\frac{h_y}{6}$ minimizing $c(\beta)$ given by (3.23), is*

$$\beta_{opt} = \frac{\frac{1}{12}(\eta^3 h_y^4 h_x^2 + 12\eta^2 h_y^4 + 144\eta h_y^2 + 24\eta^2 h_y^2 h_x^2 + 144\eta h_x^2)^{\frac{1}{2}}}{\eta h_y^2(\eta h_x^2 + 12)^{\frac{1}{2}}} - \frac{1}{4}. \tag{3.24}$$

Furthermore, $\beta_{opt} \geq 0$.

Proof The fonction f is concave : indeed its second derivative is :

$$\frac{-72\eta^2 h_y^4(\eta h_x^2+12)^2}{f^{\frac{3}{2}}}.$$

Since (g_β) is a family of affine functions coinciding with f at $t=0$, the same arguments as in proposition 2.1 imply that the minimum of $c(\beta)$ is reached in the interval $[\beta_\circ, \beta_1]$, where $\beta_\circ, \beta_1$ are defined by :

1 For all $\beta < \beta_\circ$ the graph of g_β restricted to $[0,4]$ lies under the graph of f with a sole intersection at $t=0$.

2 For all $\beta > \beta_1$ the graph of g_β restricted to $[0,4]$ lies above the graph of f with a sole intersection at $t=0$.

3 There exists a one to one decreasing mapping $\beta \to t_c(\beta)$ from $[\beta_\circ, \beta_1]$ onto $[0,4]$ such that : $g_\beta(t) \le f(t)$ for all $t \in [0, t_c(\beta)]$, $g_\beta(t) \ge f(t)$ for all $t \in [t_c(\beta), 4]$.

Note that β_1 is positive because the derivative of f at $t=0$ is positive. The sign of β_0 is that of $f(4)-f(0)$.
It is easy to check that lemma 2.1 can be applied. Therefore, $c(\beta)$ is an increasing function on $[\beta_\circ, \beta_1]$. Thus, $\beta_{opt} = max(-\frac{h_y}{6}, \beta_\circ)$. It can be checked that $\beta_\circ \ge 0$ for $\eta h_y^2 \le \frac{3}{2}$. Now, a tedious calculation yields (3.24). The proposition is proved. □

Written in terms of mass and stiffness matrices, the matrix $\tilde{S}(\beta_{opt})$ reads :

$$\tilde{S}(\beta_{opt}) = \sqrt{3(\eta h_x^2+12)}(M + (\frac{\frac{1}{12}(\eta^3 h_y^4 h_x^2 + 12\eta^2 h_y^4 + 144\eta h_y^2 + 24\eta^2 h_y^2 h_x^2 + 144\eta h_x^2)^{\frac{1}{2}}}{\eta h_y^2(\eta h_x^2+12)^{\frac{1}{2}}} - \frac{1}{12})h_y^2 L) \tag{3.25}$$

As in proposition 2.1, the condition number of $\tilde{S}(\beta_{opt})^{-1}S$ is less than the maximum of $\frac{g_{\beta_{opt}}}{f}$, which is reached at $t_\circ \in [0,4]$. However the expressions of $t_\circ$ and $\frac{g_{\beta_{opt}}}{f}(t_\circ)$ are so complicated that it is not worth writing them here. Instead, we shall give the asymptotic behaviour of $cond(\tilde{S}^{-1}S)$ in the four following asymptotic regimes

1 $h_x = r h_y$, where r is a positive parameter, and $\eta h_y^2 \to 0$. This situation corresponds to the case where the grid is refined in both directions with a fixed aspect ratio r. These kind of grids are necessary near separation point or in the zones of turbulence for example.

2 ηh_x^2 is bounded away from 0 and $\eta h_y^2 \to 0$. This kind of grid is usually used for boundary layers. The extreme case is :

3 $\eta h_x^2 \to \infty$ and $\eta h_y^2 \to 0$.

4 h_y is fixed and $\eta h_x^2 \to 0$. This is in some sense the "dual" case of 2.

For these asymptotic regimes, we shall compare the three quantities :

1 The condition number of S : $cond(S)$.

2 The condition number $cond({S_\circ}^{-1}S)$, where $S_\circ$ is the low frequency approximation of S :

$$S_\circ = h_y\sqrt{3(\eta h_x^2+12)}\left(1 + \frac{1}{2}(-\frac{1}{3} + \frac{2}{\eta h_y^2}\frac{\eta h_x^2+6}{\eta h_x^2+12})\mathcal{L}\right). \tag{3.26}$$

3 The condition number $cond(\tilde{S}(\beta_{opt})^{-1}S)$, obtained by the analysis above.

These results are summed up in the following table :

	$cond(S)$	$cond({S_\circ}^{-1}S)$	$cond(\tilde{S}(\beta_{opt})^{-1}S)$
$h_x = rh_y$, $\eta h_y^2 \to 0$	$O((\eta h_y^2)^{-\frac{1}{2}})$	$O((\eta h_y^2)^{-\frac{1}{2}})$	$O((\eta h_y^2)^{-\frac{1}{4}})$
ηh_x^2 fixed, $\eta h_y^2 \to 0$	$O((\eta h_y^2)^{-1})$	$O(1)$	$O(1)$
$\eta h_x^2 \to \infty$, $\eta h_y^2 \to 0$	$O((\eta h_y^2)^{-1})$	$\to 1$	$\to 1$
$\eta h_x^2 \to 0$, h_y fixed	$O(1)$	$O(1)$	$O(1)$

Table 3.1 Condition numbers in different asymptotic regimes

The results displayed above inspire several remarks :

Remark 3.5 The preconditioner obtained in case 1 (fixed aspect ratio)

$$\tilde{S}(\beta_{opt}) = 6M + \sqrt{3(1+r^2)}\frac{h_y}{\sqrt{\eta}}L \tag{3.27}$$

is analogous to that obtained by the continuous analysis, and yields of course the same condition number. Proposition 2.2 indicates that the condition number estimate $O((\eta h_y^2)^{-\frac{1}{4}})$ holds for a general domain decomposition. Also as for the continuous operator, the low frequency approximation of S does not improve the condition number. However in many practical cases, it turns out that the low frequency approximation of S performs well as a preconditioner.

Remark 3.6 In cases 2 and 3, carrying out the discrete analysis is crucial for improving the condition number. In these cases, the optimal preconditioner

$$\tilde{S}(\beta_{opt}) \approx \sqrt{3(\eta h_x^2 + 12)}M + \sqrt{3}\frac{h_x}{\sqrt{\eta}}L, \tag{3.28}$$

cannot be foreseen by the continuous analysis. It can be checked that the condition number obtained with the continuous analysis (2.4) is of order : $O((\eta h_y^2)^{-\frac{1}{2}})$ instead of $O(1)$ here.
The preconditioner supplied by the discrete analysis is in some sense optimal since the condition number does not depend on the mesh size.

Remark 3.7 The asymptotic regime 3 corresponds to very stretched grids : in this case, it turns out that S behaves like the matrix $I + \beta_{opt}\mathcal{L}$. This explains why both the low frequency approximation and $\tilde{S}(\beta_{opt})$ yield condition numbers converging to 1.

Important Remark 3.8 Finally, let us point out that the theoretical results in the case of high aspect ratios grids are partial, because we have not proved them in the case of an arbitrary domain decomposition.

3.3 Numerical experiments

In the following, we shall compare the Preconditioned Conjugate Gradient in Subspace $Ker(B)$ (called PCGS) with preconditioner

$$\begin{pmatrix} \tilde{S} & B^T \\ B & 0 \end{pmatrix},$$

with the same method with preconditioner

$$\begin{pmatrix} I & B^T \\ B & 0 \end{pmatrix}. \tag{3.29}$$

In fact, this matrix is not used to improve the condition number, but only to permit a conjugate gradient in subspace $Ker(B)$. Thus, we shall refer to this method as CGS.

3.3.a The test problem.

For this set of experiments, the domain Ω is the approximation of the exterior of a circular body. In fact, this case is a rather realistic one, because, as we shall see, it forbids uniform meshes as studied in the theoretical paragraphs above. Thus, the formulas given above will not be used in a straightforward manner.
The boundary $\partial\Omega$ can be divided into two connected parts : the body's wall Γ_0 and the outer boundary Γ_∞.
Since exactly polygonal subdomains are much easier to treat than curved ones (in the first case isoparametric finite elements are needed whereas the second case requires overparametric finite elements), the subdomains should be preferably polygonal. For this reason, we set Γ_∞ to be piecewise polygonal. Therefore, the domain decomposition is designed so that every subdomain Ω_k is a polygonal, unless $\partial\Omega_k \cap \Gamma_0 \neq \emptyset$. In that case, $\partial\Omega_k$ is made of three straight segments and a curved line. The following figure represents an exemple of domain decomposition :

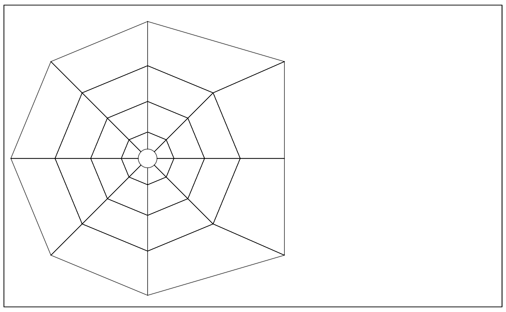

Figure 3.1 : an example of domain decomposition :
every subdomain Ω_k is polygonal, except if $\partial\Omega_k \cap \Gamma_0 \neq \emptyset$.

Let T_k map the unit square into Ω_k. The construction of T_k is rather simple when Ω_k is polygonal, (isoparametric transformation given by 6 parameters per subdomain). When Ω_k is curved, and $\partial\Omega_k$ has 3 straight segments, T_k is the composition of an affine transformation on a curved line and of the previously described isoparametric transformation (see fig 3.2).

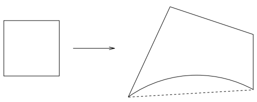

Figure 3.2 : the transformation T^k if $\partial\Omega_k \cap \Gamma_0 \neq \emptyset$.

For each subdomain Ω_k, a fine grid $\mathcal{T}_{k,h}$ is built in the following way : in the unit square, we construct a structured mesh, fully described by a few parameters : here, we use finite difference grids. Each quadrangle is divided into $nx \times ny$ smaller quadrangles. These divisions are made with parallel lines in the frame of reference where the quadrangle is a unit square (isoparametric mapping unless one border is curved). However the division is not uniform : in each subdomain, two aspect ratio are given so as to refine near one boundary in each direction: ρ_x, ρ_y . The mesh size increases geometrically from dx to $dx\rho_x$ from one cell to the next going West to Est and similarly in y northbound; To summarize, for each subdomain Ω_k, the mesh in the reference frame is described by the four parameters : nx, ny, ρ_x, ρ_y.

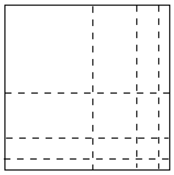

Figure 3.3 : Exemple of a mesh in the reference frame

Then this mesh is mapped into Ω_k by means of T_k. The meshes need not match at subdomains' interfaces. Therefore, this yields a nonconforming mesh for Ω with a few parameters only. Isoparametric Q_1 finite elements are used in subdomains Ω_k such that $\partial\Omega_k \cap \Gamma_0 = \emptyset$. On the contrary, if an edge of $\partial\Omega_k$ is supported by Γ_0, then we use overparametric Q_1 finite elements.

3.3.b Stretched grids

The first experiment deals with stretched grids, often used for treating laminar boundary layers. The domain is roughly speaking the ring $1 \le r \le 2.4$. There are 16 subdomains disposed in two concentric layers ($1 \le r \le 1.7$ and $1.7 \le r \le 2.4$) of 8 subdomains each. Each subdomain occupies an angular sector of $\frac{\pi}{4}$. In this case, nx (resp. ny) stands for the number of steps in the polar (resp. radial) direction. For all subdomains, the parameters nx, ny, ρ_x, ρ_y are the same :

for mesh 1,

$$nx = 10, \quad ny = 70, \quad \rho_x = 1, \quad \rho_y = 1.$$

For mesh 2

$$nx = 5, \quad ny = 70, \quad \rho_x = 1, \quad \rho_y = 1.$$

Such meshes, rather unrealistic, are designed to exhibit rather large aspect ratio : indeed, in the first layer of mesh 1, the aspect ratio varies beetween 7.8 and 13.3. In the first layer of mesh 2, the aspect ratio varies beetween 15 and 27. This kind of grids can describe boundary layers effects correctly up to $\eta \approx 300$.

Of course, the subdomains are not rectangles nor the grids uniform. Since the subdomains are not rectangles, the grids are not orthogonal to their boundary. Let Ω_k be a generic subdomain. The preconditioner is derived by making the approximation that at each point of $\partial\Omega_k$ the grid is locally uniform. Since the grid is not necessarily orthogonal to $\partial\Omega_k$, the formulas used for the preconditioner are not those established in §3.2, but are derived from Remark 3.3 concerning oblique grids.

For the experiment below, the stopping criteria of the iterative methods is :

$$\frac{\alpha_i}{\alpha_1} < 10^{-12},$$

where α_i is the residual at iteration i.

The following table presents the performances of the method PCGS compared to those of CGS.

	$\eta = 200$	$\eta = 100$	$\eta = 50$
mesh 1, CGS	89	99	113
mesh 1, PCGS	11	19	30
mesh 2, CGS	108	126	151
mesh 2, PCGS	9	17	26

Table 3.2 Performances of the algorithms CGS and PCGS for stretched meshes.

Note that the preconditioner's efficiency decreases with η. This does not contradict the asymptotics of table 3.1, because as η decreases, the contribution of ηh_x^2 to the condition number is no longer negligible.
The table also seems to indicate that the efficiency of the preconditioner increases along with the aspect ratio. This phenomenon was predicted in table 3.1.
The convergence histories for mesh 1 and $\eta = 100$ are displayed on next figure :

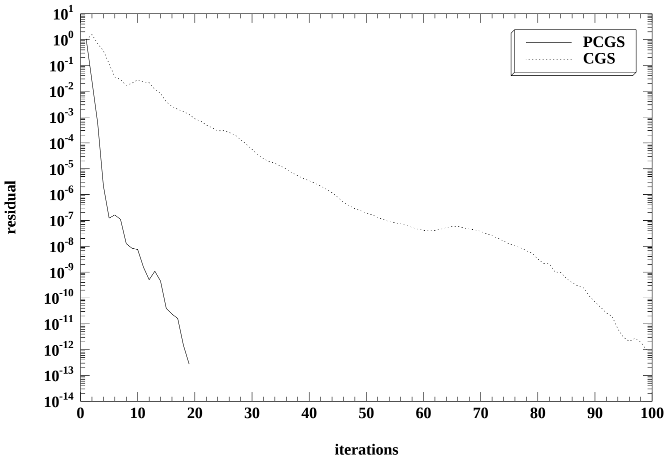

Figure 3.4 Convergence for mesh 1 and $\eta = 100$.

These performances should also be compared to that of the unpreconditioned Uzawa algorithm, (see table 4.2 and figure 4.1 below). For instance, for mesh 1 and $\eta = 100$, the convergence of the Uzawa algorithm is obtained in around 250 iterations.

3.3.c A practical case.

The mesh used in the following experiment has already been used in [2], for computing a Navier Stokes flow around an infinite cylinder at Reynolds number 100. Its main features are :

1 The domain decomposition is made of 4 concentric layers of eight subdomains each.

2 Near the body, the mesh is refined : the mesh steps in the radial direction form a geometrical progression, with ratio $\rho_y = 1.1$. The other characteristics of the mesh in the first layer near the body are

$$nx = 30, \quad ny = 40, \quad \rho_x = 1.$$

3 In the other layers of subdomains away from the body : the mesh is rather coarse :

$$nx = 10, \quad ny = 10, \quad \rho_x = 1, \quad \rho_y = 1.$$

Hence, the meshes do not match at the interface beetween the first and second layer of subdomains.

4 In the region corresponding to the wake of the flow behind the body, the mesh is refined in the y direction. A part of the mesh is shown on next figure :

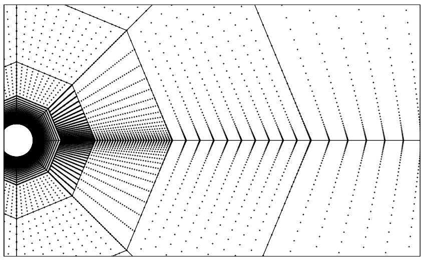

Figure 3.5 Mesh 3.

The radius of the inner circle is 1, and we shall test the preconditioner for $\eta = 200$ and $\eta = 800$.

Such a mesh displays many asymptotical regimes : near the body, the aspect ratios are rather high. Away, from the body, the mesh is coarse. Finally, in intermediate regions, the mesh is fine with aspect ratios close to one.

For $\eta = 200$ the method PCGS (resp.CGS) converges in 9 iterations, (resp. 40). For $\eta = 800$ the method PCGS (resp.CGS) converges in 8 iterations, (resp. 57), as shown by the figure below:

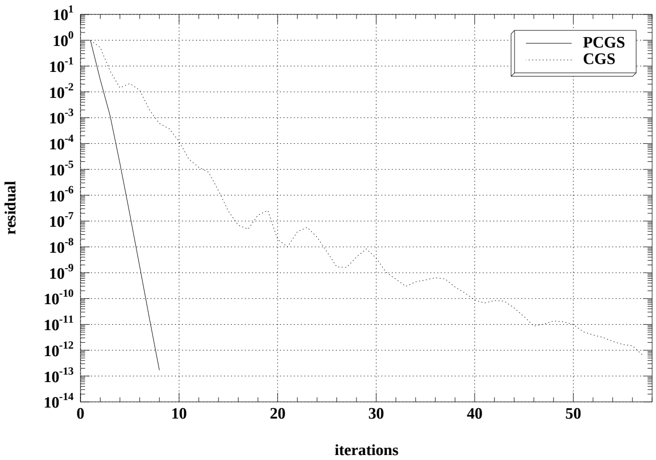

Figure 3.6 Convergence for mesh 3 and $\eta = 800$.

4. ANOTHER STRATEGY : CHOOSING OTHER JUMP OPERATORS

In sections 2 and 3, the idea was to approximate the discrete Steklov Poincaré operator S_h by a local operator $\tilde{S}_h$. Once $\tilde{S}_h$ is found, one can either use a preconditioned conjugate gradient method, *i.e* an iterative algorithm performing at each step the product of a vector by matrix :

$$\begin{pmatrix} \tilde{S} & B^T \\ B & 0 \end{pmatrix}^{-1} \begin{pmatrix} S & B^T \\ B & 0 \end{pmatrix},$$

or a preconditioned Uzawa method, *i.e* each time steps involves the product of a vector by

$$\left(B\tilde{S}^{-1}B^T\right)^{-1} BS^{-1}B^T.$$

Of course, the matrix $\left(B\tilde{S}^{-1}B^T\right)^{-1}$ is not computed in practice. Instead, the basis of both algorithms is the resolution of the linear system

$$B\tilde{S}^{-1}B^T\Lambda = \Psi. \tag{4.1}$$

The matrix $\tilde{S}$ has been chosen in such a way that (4.1) can be solved in quite an efficient and unexpensive way (see [1]). However, the algorithm used to solve (4.1) requires a rather important programming effort.

The aim of this section is to suggest a possible improvement of the domain decomposition method which would not be based on preconditioning but rather on choosing a new jump operator $\tilde{B}_h$ instead of B_h, so that $\tilde{B}S^{-1}\tilde{B}^T$ is *already* better conditioned than $BS^{-1}B^T$. The advantage of such a method is that it does not require any additional programming work, and it may save the use of a preconditioner in some cases. However, for the special class of $\tilde{B}_h$ considered in this section, we shall see that it is not possible to reduce the condition number as much as by using the preconditioners described in §2 and §3. Another and very important limitation of the ideas presented below is that they require that the grids on the two sides of each interface Γ_{kl} have roughly the same characteristics.

Roughly speaking, for an interface Γ_{kl}, the idea is to consider $\alpha_{kl}(s)[u] - \frac{d}{ds}\beta_{kl}(s)\frac{d[u]}{ds}$ instead of $[u]$, where α_{kl} and β_{kl} are two positive functions on Γ_{kl}, which shall be constant if the grids are uniform in Ω_k and Ω_l. The aim of the section is to show that choosing suitably α_{kl} and β_{kl} may decrease the condition number of $\tilde{B}S^{-1}\tilde{B}^T$.

To be more precise, let us call $\tilde{b}_h$ the bilinear form on $X_h \times W_h$

$$\tilde{b}_h(\mathbf{v}_h, \mu_h) = \sum_{1\le k<l\le K} \int_{\Gamma_{kl}} \alpha_{kl}(Tr_k v_{h,k} - Tr_l v_{h,l})\mu_h + \beta_{kl}\frac{\partial}{\partial s}(Tr_k v_{h,k} - Tr_l v_{h,l})\frac{\partial}{\partial s}\mu_h. \tag{4.2}$$

We associate to $\tilde{b}_h$ the linear operator $\tilde{B}_h$ from X_h to W_h such that $\tilde{b}_h(\mathbf{v}_h, \mu_h) = (\tilde{B}_h\mathbf{v}_h, \mu_h)$. Calling $\tilde{Y}_h$ the space :

$$\tilde{Y}_h = \left\{\mathbf{v}_h \in X_h \text{ such that } \quad \tilde{B}_h\mathbf{v}_h = 0\right\},$$

the domain decomposition problem becomes : find $\mathbf{u}_h \in \tilde{Y}_h$ such that

$$\forall \mathbf{v}_h \in \tilde{Y}_h, \quad \sum_{k=1}^K \int_{\Omega_k} \nabla u_{h,k} \cdot \nabla v_{h,k} + \eta \sum_{k=1}^K \int_{\Omega_k} u_{h,k}\, v_{h,k} = \sum_{k=1}^K \int_{\Omega_k} f\, v_{h,k}. \tag{4.3}$$

It can be checked that problem (4.3) is well posed.

Remark No numerical analysis of (4.3) exists so far. In our experiments (see §4.2), we have not noticed any loss of accuracy with this kind of method. However a careful numerical analysis may suggest a special treatment of crosspoints.

Remark The choice of $\tilde{b}_h$ in the class (4.2) is motivated by the use of low order finite elements. For higher order finite elements, higher order positive jump operators may be considered.

Problem (4.3) admits the following saddle point formulation : find $(\mathbf{u}_h, \lambda_h) \in X_h \times W_h$ such that

$$\begin{aligned} A_h \mathbf{u}_h + \tilde{B}_h^T \lambda_h &= f_h, \\ \tilde{B}_h \mathbf{u}_h &= 0. \end{aligned} \tag{4.4}$$

Finally a Schur complement method yields a linear system of the form :

$$\begin{pmatrix} S & \tilde{B}^T \\ \tilde{B} & 0 \end{pmatrix} \begin{pmatrix} V \\ \Lambda \end{pmatrix} = \begin{pmatrix} P \\ 0 \end{pmatrix}. \tag{4.5}$$

The question is how to choose α_{kl} and β_{kl} in (4.2). As above, we shall consider a model case involving uniform grids.

4.1 A model case

The model case is similar to that of §3.1 except that the grids on both side of Γ are the same :

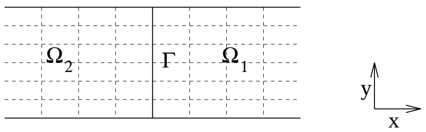

Figure 4.1 : the model case

The matrix $\tilde{B}$ can be written

$$\tilde{B} = \tilde{B}_1 + \tilde{B}_2,$$

where $\tilde{B}_1 : Z_{1h} \rightarrow W_h$ and $\tilde{B}_2 : Z_{2h} \rightarrow W_h$. Thus, the matrix $\tilde{B}S^{-1}\tilde{B}^T$ reads :

$$\tilde{B}S^{-1}\tilde{B}^T = \tilde{B}_1 S_1^{-1} \tilde{B}_1^T + \tilde{B}_2 S_2^{-1} \tilde{B}_2^T,$$

where S_1 (resp. S_2) is the matrix related to the discrete Steklov Poincaré in subdomain Ω_1 (resp. Ω_2).
By symmetry, it is obvious that $\tilde{B}_1 = \tilde{B}_2$ and $S_1 = S_2$. Therefore, the aim is to choose $c_\circ$ and c_1 minimizing the condition number of $\tilde{B}_1 S_1^{-1} \tilde{B}_1^T$, with

$$\tilde{B}_1 = c_\circ M + c_1 L \tag{4.6}$$

Thanks to (3.14),(3.19), searching $\tilde{B}_1(\beta)$ in the form :

$$\tilde{B}_1(\beta) = (\frac{3(\eta h_x^2 + 12)}{h_y^2})^{\frac{1}{4}} (M + (\beta + \frac{1}{6}) h_y^2 L) \tag{4.7}$$

is equivalent to finding $\beta \geq -\frac{h_y}{6}$ minimizing :

$$\frac{\underset{1\leq n\leq N-1}{max} \frac{g_\beta}{f}(l_n)}{\underset{1\leq n\leq N-1}{min} \frac{g_\beta}{f}(l_n)}, \tag{4.8}$$

where (l_n) is given by (3.15), f is given by (3.17), and where

$$g_\beta(l_n) = (1+\beta l_n)^2. \tag{4.9}$$

As in §2.2,§3.2 the minimum of this discrete problem is smaller than that of the continuous one : find $\beta_{opt} \geq -\frac{h_y}{6}$ minimizing $c(\beta)$:

$$c(\beta) = \frac{\underset{0\leq t\leq 4}{max} \frac{g_\beta}{f}(t)}{\underset{0\leq t\leq 4}{min} \frac{g_\beta}{f}(t)}. \tag{4.10}$$

The following proposition stems from lemma 2.1 :

Proposition 4.1 *Assume $h_y^2\eta \leq \frac{3}{2}$, then $\beta_{opt} \geq -\frac{h_y}{6}$ minimizing $c(\beta)$ given by (4.9), is :*

$$\beta_{opt} = \frac{1}{4}\left(\frac{1}{9}\frac{\eta^3 h_y^4 h_x^2 + 12\eta^2 h_y^4 + 24\eta^2 h_y^2 h_x^2 + 144\eta h_y^2 + 144\eta h_x^2}{\eta^2 h_y^4(\eta h_x^2+12)}\right)^{\frac{1}{4}} - \frac{1}{4}. \tag{4.11}$$

Furthermore, $\beta_{opt} \geq 0$.

Proof The proof is exactly the same as for proposition 3.1. It is enough to verify that the family g_β satisfies all the hypothesis of lemma 2.1. With the notations of lemma 2.1, the optimum is reached at $max(-\frac{h_y}{6}, \beta_\circ)$. The expression of $\beta_\circ$ follows from computations, and it can be checked that for $h_y^2\eta \leq \frac{3}{2}$, $\beta_\circ \geq 0$. □

Written in terms of mass and stiffness matrices, $\tilde{B}_1(\beta_{opt})$ is

$$\tilde{B}_1(\beta_{opt}) =$$
$$\frac{(3\eta h_x^2+36)^{\frac{1}{4}}}{h_y^{\frac{1}{2}}}\left(M + (\frac{1}{4}(\frac{1}{9}\frac{\eta^3 h_y^4 h_x^2 + 12\eta^2 h_y^4 + 24\eta^2 h_y^2 h_x^2 + 144(\eta h_y^2 + \eta h_x^2)}{\eta^2 h_y^4(\eta h_x^2+12)})^{\frac{1}{4}} - \frac{1}{12})h_y^2 L\right) \tag{4.12}$$

As above we shall not express the condition number in the general case, because it is too complicated. Instead, we shall focus on asymptotic regimes, and we shall compare the condition number to that of $B_1^T S_1^{-1} B_1$, and to that of $\tilde{B}_{1\circ}^T S_1^{-1} B_{1\circ}$, where $\tilde{B}_{1\circ}$ corresponds to a low frequency approximation :

$$\tilde{B}_{1\circ} = (\frac{3(\eta h_x^2+12)}{h_y^2})^{\frac{1}{4}}(M + (\frac{h_y^2}{6} + \frac{1}{2\eta}\frac{\eta h_x^2+6}{\eta h_x^2+12})L).$$

These results are summed up in the following table :

condition number of	$B_1^T S_1^{-1} B_1$	$\tilde{B}_{1\circ}^T S_1^{-1} \tilde{B}_{1\circ}$	$\tilde{B}_1^T(\beta_{opt}) S_1^{-1} \tilde{B}_1(\beta_{opt})$
$h_x = rh_y$, $\eta h_y^2 \to 0$	$O((\eta h_y^2)^{-\frac{1}{2}})$	$O((\eta h_y^2)^{-\frac{3}{2}})$	$O((\eta h_y^2)^{-\frac{3}{8}})$
ηh_x^2 fixed, $\eta h_y^2 \to 0$	$O((\eta h_y^2)^{-1})$	$O((\eta h_y^2)^{-1})$	$O((\eta h_y^2)^{-\frac{1}{2}})$
$\eta h_x^2 \to \infty$, $\eta h_y^2 \to 0$	$O((\eta h_y^2)^{-1})$	$O((\eta h_y^2)^{-1})$	$O((\eta h_y^2)^{-\frac{1}{2}})$
$\eta h_x^2 \to 0$, h_y fixed	$O(1)$	$O(1)$	$O(1)$

Table 4.1 Condition numbers in different asymptotic regimes

Remark 4.1 The gains in condition number are smaller than those obtained in §3. The main reason for this is that in §3, the symbol of S was approached by a linear function; here, it is approached by the square of a linear function. Although the gains are smaller, the idea of choosing other jump operators than B_h is interesting, because it does not require additional programming work and CPU time.

Remark 4.2 It is possible to combine the approaches of choosing other jump operators than B_h, namely $\tilde{B}_h$, and of the preconditioned gradient in subspace $Ker(\tilde{B})$. This should improve the condition numbers obtained in §3.

Remark 4.3 Note that the low frequency approximation worsens the condition number in the case of uniformly refined meshes, and does not improve it in the case of stretched grids.

4.2 Numerical experiments

In this paragraph, we shall compare the performances of the Uzawa algorithm with B (corresponding to the usual jump operator), $\tilde{B}_{opt}$ (computed interface by interface, with formula (4.11)), and $\tilde{B}_\circ$, corresponding to the low frequency approximation.
As above, two different test cases will studied, the first one for stretched meshes and the second for uniformly refined meshes.

4.2.a Stretched meshes

For this experiment, it is possible to use meshes 1 and 2, because the grids are similar on both sides of each interfaces.
The following table gives the performances of the Uzawa algorithm, with the three jump operators.

	$\eta = 200$	$\eta = 100$	$\eta = 50$
mesh 1, B	256	278	324
mesh 1, $\tilde{B}_{opt}$	40	46	56
mesh 1, $\tilde{B}_\circ$	58	89	144
mesh 2, B	262	332	348
mesh 2, $\tilde{B}_{opt}$	45	51	55
mesh 2, $\tilde{B}_\circ$	51	80	124

Table 4.2 Performances for stretched meshes.

For this kind of mesh, using $\tilde{B}_{opt}$ instead of B permits to reduce the computation cost by a factor at least 6. The difference beetween the solutions of the two problems (with $\tilde{B}_{opt}$ and B) is less than 10^{-6} in L^∞ norm.
Note that the efficiency of the algorithm with $\tilde{B}_\circ$ decreases very fast as η decreases, much faster than that of $\tilde{B}_{opt}$. This may be explained by saying that as η decreases, the contribution of ηh_x^2 cease being negligible and worsens very fast the condition number.

The convergence histories for mesh 1 and $\eta = 100$ are displayed on next figure :

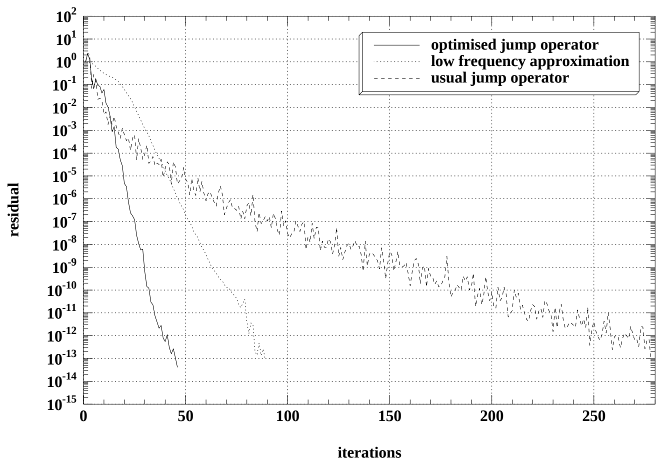

Figure 4.1 Convergence for mesh 1 and $\eta = 100$.

4.2.b Uniformly refined meshes.

In this experiment the domain is the rectangle $[-0.5, 0.5] \times [-0.25, 0.25]$. It is divided in 4×2 squares of side 0.25. In each square, there is a uniform square mesh, whose step size is $1/160$. The Uzawa algorithms were tested for $\eta = 400$ and $\eta = 200$.
The table below presents the performances of the Uzawa algorithm, with the three jump operators.

	$\eta = 400$	$\eta = 200$	$\eta = 50$
mesh 4, B	40	42	43
mesh 4, $\tilde{B}_{opt}$	16	17	20
mesh 4, $\tilde{B}_\circ$	114	161	349

Table 4.3 Performances for mesh 4.

The theoretical calculations of table 4.1. explain very well why the low frequency approximation $\tilde{B}_\circ$ performs very poorly.
The convergence histories for mesh 4 and $\eta = 400$ are displayed on next figure :

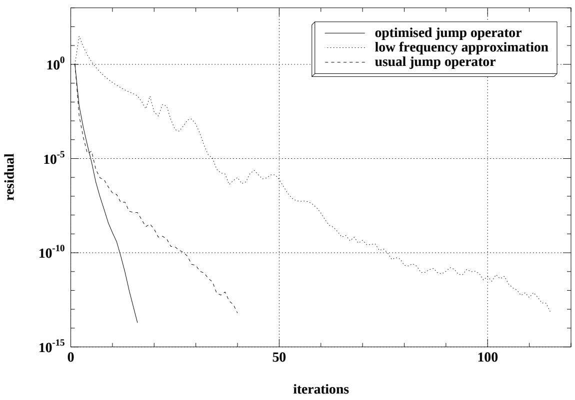

Figure 4.2 Convergence for mesh 4 and $\eta = 400$.

This figure shows that the idea of choosing other jump operators may not be sufficient to increase significantly the efficiency of the method in the case of uniformly refined grids.

Conclusion

Two possible ideas for accelerating iterative methods for solving (1.13) have been proposed. Both of them lie on approximating the Steklov Poincaré operator on subdomains by local differential operators.
The first one consists in using a preconditioned conjugate gradient for (1.20) in the kernel of B. When the meshes are uniformly refined, a continuous analysis can be used to guess the optimal preconditioner in the considered class. In the frequent case when the meshes exhibit high aspect ratios, then a discrete analysis is necessary to build an efficient preconditioner. Numerical tests have been carried out on realistic situations. They demonstrate the efficiency of this approach.
The second idea, rather new to our knowledge, applies to the cases when mesh characteristics do not vary too much across subdomains interfaces. Such an approach is somehow related to the techniques of absorbing boundary conditions and consists in choosing a higher order jump operator B. Although this method cannot be applied in all situations, and the gain in condition number is not as important as for the first approach, it is interesting because it does not require additional programming work. Numerical tests give promising results in the case of high aspect ratios meshes.

Bibliography

[1] Y. Achdou, Yu.A. Kuznetsov, O.Pironneau, in preparation.
[2] Y. Achdou, O.Pironneau, *A fast solver for Navier-Stokes equations in the laminar regime using mortar finite element and boundary element method.*, to appear in SIAM j. of Numerical Analysis.
[3] V.K.Agapov, Yu.A. Kuznetsov. *On some versions of the domain decomposition methods.* Soviet J. of Num. Anal. and Math. modelling , 1988-3, pp 245-266.
[4] F.Ben Belgacem, Y. Maday, *A non conforming finite element method with application to parallel implementations* , submitted to M^3AS, (1993). See also F.Ben Belgacem *The mortar finite element method with Lagrange multipliers*, to appear.
[5] C.Bernardi. *Relèvement de traces dans les espaces d'éléments finis* unpublished
[6] C. Bernardi, Y. Maday, A. Patera, *A new nonconforming approach to domain decomposition : the mortar element method* , Nonlinear partial differential equations and their applications, Pitman, H. Brezis, J.L. Lions eds. (1989).
[7] C.Bernardi,Y. Maday, G. Sacchi Landriani. *Nonconforming matching conditions for coupling spectral and finite element methods* Applied Numerical Mathematics 6 pp 65-84 (1989/90).
[8] J.F. Bourgat, R. Glowinski, P. Le Tallec, M. Vidrascu,*Variational Formulation and Algorithm for Trace Operator in Domain Decomposition Calculations.* in T.F Chan et al. eds., Second International Symposium on Domain Decomposition Methods for Partial Differential Equations, pp3-17, Philadelphia, 1989.
[9] F. Brezzi, L.D. Marini, *A three field domain decomposition method* , Contemporary Mathematics 157. pp27-34 (1994).
[10] T.Chan. *Analysis of preconditioners for domain decomposition*, SIAM j. of Numerical Analysis, 24-2 (1987). pp382-390.
[11] B.Engquist, A.Majda, *Absorbing boundary conditions for the numerical simulations of waves* Math. Comp. 31(139), (1977). pp629-651.

[12] R. Glowinski, O.Pironneau, *Numerical methods for the first biharmonic equation and for the two dimensional Stokes problem.*, SIAM Review 21, No2, (1979) pp.167-212.

[13] Yu.A. Kuznetsov, G.I.Marchuk. *Méthodes itératives et fonctionelles quadratiques*, Méthodes Mathématiques de l'Informatique-4 : sur les méthodes numériques en Sciences physiques et économiques. (J.L. Lions ,G.I.Marchuk eds) pp 3-132, Dunod, Paris, 1974.

[14] P.Le Tallec, T. Sassi. *Domain decomposition with non matching grids*, INRIA report (1991) .

[15] F.Nataf, F. Rogier.*Factorization of the convection diffusion operator and the Schwarz algorithm.* To appear in M^3AS.

[16] O.Widlund. *An extension theorem for finite element spaces with three applications* in W.Hackbush, K. Witdr eds, Numerical techniques in Continuum mechanics. Kiel (1986).

APPENDIX

We give the proof of
Lemma 3.1
Assume $\min(h_x, h_y) < \sqrt{\frac{6}{\eta}}$ *and let* $C_\circ = -\log(5(1-\sqrt{1-\frac{1}{25}})) \sim 2.29$ *then,*

1 $h_x > \sqrt{\frac{6}{\eta}} \Rightarrow e^{-z_n \frac{D}{h_x}} \leq e^{\frac{-D}{h_x} C_\circ}$.

2 $h_x < \sqrt{\frac{6}{\eta}} \Rightarrow \exists c > 0$ *independant of* h_x, h_y *and* $\sqrt{\eta}$, *such that* $e^{-z_n \frac{D}{h_x}} \leq e^{-\sqrt{\eta} D c}$

proof From (3.12), $e^{-z_n} = \frac{S_0^n}{2S_1^n}(-1+\sqrt{1-\frac{4{S_1^n}^2}{{S_0^n}^2}})$. Let $\alpha(l_n) = \frac{S_0^n}{|2S_1^n|} - 1$, we have $0 \leq \alpha$ and

$$|e^{-z_n}| = (1+\alpha)(1-\sqrt{1-\frac{1}{(1+\alpha)^2}}) = f(\alpha)$$

It can be checked that $f'(\alpha) \leq 0$.
Let us introduce the function S_1 defined by $S_1(l_n) = S_1^n$. It is easy to see that $S_1(l_n)$ is an increasing function of l_n since $\min(h_x, h_y) < \sqrt{\frac{6}{\eta}}$.
• If l_n is such that $S_1^n \leq 0$, $\alpha(l_n) = \frac{S_0^n + 2S_1^n}{-2S_1^n}$. It can be checked that $\alpha'(l) > 0$. Thus, we have $\alpha(l_n) \geq \alpha(0) = \frac{3}{\frac{6}{\eta {h_x}^2} - 1}$ and thus $f(\alpha) \leq 1 - \frac{-3\eta {h_x}^2 + 6\sqrt{\eta} h_x \sqrt{1+\eta {h_x}^2/12}}{6-\eta {h_x}^2}$. By using the inequality $(1-x)^p \leq e^{-px}$ with $p = \frac{D}{h_x}$, we have $|e^{-z_n}|^{\frac{D}{h_x}} \leq e^{-\sqrt{\eta} D (\frac{3\sqrt{\eta} h_x - 6\sqrt{1+\eta {h_x}^2/12}}{6-\eta {h_x}^2})}$. It can be checked that the term $\frac{3\sqrt{\eta} h_x - 6\sqrt{1+\eta {h_x}^2/12}}{6-\eta {h_x}^2}$ is bounded from below by a positive constant c. This gives $|e^{-z_n}|^{\frac{D}{h_x}} \leq e^{-\sqrt{\eta} D c}$.
• If l_n is such that $S_1^n \geq 0$, $\alpha(l_n) = \frac{S_0^n - 2S_1^n}{2S_1^n}$. It can be checked that $\alpha'(l) < 0$. Thus, we have $\alpha(l_n) \geq \alpha(4) \geq 4$. We have $f(4) = 5(1-\sqrt{1-\frac{1}{25}})$. This gives $|e^{-z_n}|^{\frac{D}{h_x}} \leq e^{\frac{D}{h_x}\log(5(1-\sqrt{1-\frac{1}{25}}))}$.

We can now conclude. If $h_x < \sqrt{\frac{1}{\frac{2}{h_y^2}+\frac{\eta}{6}}}$, it can be checked that $S_1(0) \leq S_1(4) \leq 0$ and thus estimate **1** holds. If $h_x > \sqrt{\frac{6}{\eta}}$, it can be checked that $S_1(0) \geq 0$ and thus, $S_1^n \geq 0$. Thus, estimate **2** holds. In the intermediate case, $\sqrt{\frac{1}{\frac{2}{h_y^2}+\frac{\eta}{6}}} < h_x < \sqrt{\frac{6}{\eta}}$, we have $S_1(0) \leq 0 \leq S_1(4)$. Thus, $\exists l_*$ s.t.

$$0 \leq l_n \leq l_* \Rightarrow S_1^n \leq 0 \Rightarrow e^{-z_n \frac{D}{h_x}} \leq e^{-\sqrt{\eta} D c}$$

and

$$l_* \leq l_n \leq 4 \Rightarrow S_1^n \geq 0 \Rightarrow e^{-z_n \frac{D}{h_x}} \leq e^{\frac{-D}{h_x} C_\circ} \leq e^{-\sqrt{\eta} D \frac{C_\circ}{\sqrt{6}}}.$$

Thus, by taking $c = \min(c, \frac{C_\circ}{\sqrt{6}})$, estimate **1** holds. □